Title	Fabrication of Reactive Polymethacrylate Monoliths via Thermally Induced Phase Separation and Their Applications
Author(s)	Han, Wenjuan
Citation	大阪大学, 2014, 博士論文
Version Type	VoR
URL	https://doi.org/10.18910/52147
rights	
Note	

Doctoral Dissertation

Fabrication of Reactive Polymethacrylate Monoliths *via* Thermally Induced Phase Separation and Their Applications

（熱誘起相分離を利用した反応性アクリル樹脂モノリスの作製と応用）

Wenjuan Han

October 2014

Graduate School of Engineering
Osaka University

Contents

Page

Chapter 1

Fabrication and Characterization of PGM Monolith *via* Thermally Induced Phase Separation

Chapter 2

Immobilization of horseradish peroxidase on modified PGM monolith

Chapter 3

Pepsin immobilization on an aldehyde-modified polymethacrylate monolith and its application for protein analysis

General Introduction

In nature, monolith is not a new word. Generally speaking, “monolith" means a large block of stone according to the definition in the Webster’s College Dictionary. The monolith in Australia (Fig. 1A) is probably the largest one in the world. In the field of materials science and engineering, a monolith is often regarded as a single-piece bulk material having three-dimensionally developed continuous pores. During the two to three decades of development, monoliths are considered as the most promising material for both academic and industry due to their unique characterization and various fabrication methods [1-5].

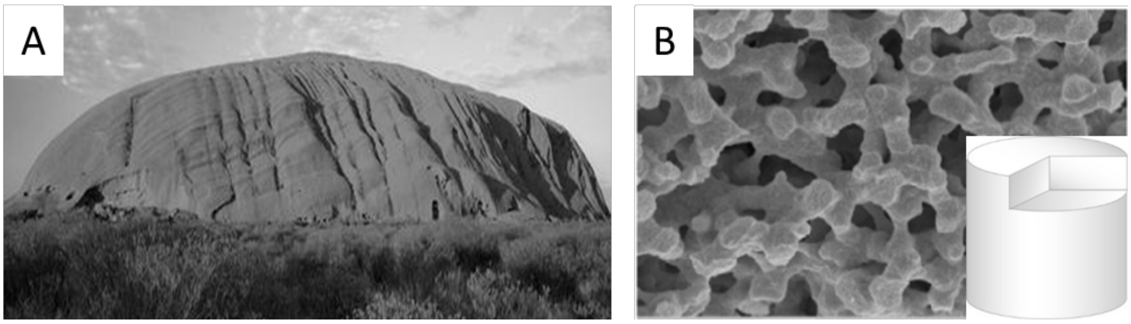

Fig. 1 Examples of monoliths (A) in nature (The Ayers Rock in Australia) and (B) in the field of materials science and engineering

The term of monolith was first introduced by Svec and Frechet as continuous porous structure fabricated through copolymerization from glycidyl methacylate and ethylene dimethacylate mixed with porogenic solvents in a mold [6]. The history of monolith could be traced back to the idea of Nobel Prize winner Robert Synge who first postulated a “continuous block of the porous gel structure” as stationary phase in chromatograph in 1952 [7]. However, he realized that such soft materials available at that time for such device would collapse under hydrostatic pressure. In the early 1970s, polyurethane foams were prepared in situ within the confines of large chromatographic column, and decent separations could be obtained in gas chromatography and liquid chromatography [8-10]. Nevertheless, none of these early technologies lasted long, and the modern era of monolith began much later. After the initial efforts, Hjerten et al. showed that it is possible to form a macroporous polymer matrix inside a chromatographic tube and acceptable backpressure can be achieved at moderate flow rates in 1989 [11]. Svec and Frechet prepared an interconnected porous polymer rod by in situ polymerization of glycidyl methacrylate and ethylene dimethacrylate in presence of porogenic solvents inside a chromatographic tube, which was the birth of a separation medium called monolith [6].

Compared to other porous media such as porous particles and porous membranes that are also commonly employed, monolith is featured by outstanding characteristics such as high capacity due to large surface area, fast mass transfer based on low pressure loss, high resolution due to uniform structure without void, various matrix polymers, easy chemical modification to immobilize functional groups and high stability [12-18]. As a result, monoliths have been applied in numerous areas.

Monoliths are widely used in chromatography and considered as the fourth-generation chromatography materials as soon as its emergence in the late 1980s and early 1990s to be used first as stationary phases in high performance liquid chromatography [19-21]. Recently, monoliths have consolidated their position in separation, since more than thousands of applications have been reported in the past couples of decades and their advantages of monolith compared to conventional chromatography demonstrated. It is well known that the conventional chromatography with porous particles is widely used in separation field especially for small molecule

[22-26]. However, there are always large void volumes remained inside the particle-packed column because of the particulate character of packing process, leading to a significant invalid part of the column for separation. In addition, the separation rate for large molecules in particle-packed column is always slow due to the low mass transfer and high back pressure problems [15-18]. In contrast to the column with packed particles, monolith with continuous interconnected pores in a whole piece results in good permeability and mass transfer which provides a high flow rate at a moderate back pressure. As a result, the applications of monolith in a variety of chromatographic mode, including gas chromatography, HPLC and capillary electrochromatography have been widely used because of their small-sized skeletons and wide through-pores much higher separation efficiency can be achieved than the case with particle-packed columns at a similar pressure. Moreover, monoliths are applied as an ideal candidate to separate large molecules such as proteins, peptides, cells, oligo- and polynucleotides, polymer-supported reagents and scavengers [27-31]. Recently, monoliths are widely applied for liquid chromatography, capillary chromatography, solid-phase extraction SPE and thin layer chromatography [32-39].

Monolith also can be used as supports for catalyst [40-45]. Essential to all supported catalysts is the reservation of sufficient reaction rates, high activities, simplicity of preparation, extraction and recycling of the catalyst, and contamination or metal leaching in the products. Even though porous catalytic support besides monolithic media have suffered from lowed catalytic activity compared with that of unbound catalysts in solution, the use of monoliths posed an advantage over other porous structure. Their large flow-through pores, which contribute to significant mass transfer, also prevent the reactions from being only diffusion controlled [46-48]. Monolith support for metathesis catalysts, Cu-based catalysts for carbonyl hydrosilylations and hydrocyanations, Pd-based catalysts for C-C coupling reactions are investigated. Fig. 2 shows an example of immobilization of Schrock-type catalysts on monolith [49].

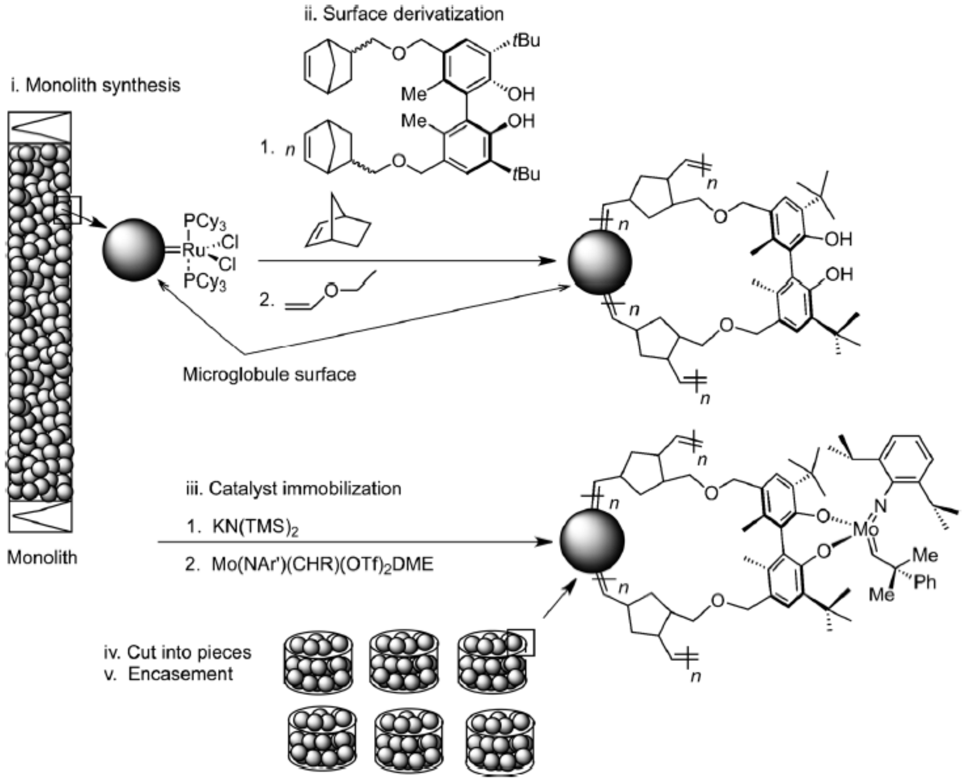

Fig. 2 Example of immobilization of Schrock-type catalysts on monolith [49]

Application of the monolith with 3-dimentional interconnected pores as cell scaffolds with functions, such as providing structure support, serving as a substrate for cell attachment, is investigated [50-54]. Due to the internal characteristic with large pore size and improved mechanical stability, monolith is a promising matrix for cell scaffolds which is typically open, large pore size structures. For example, Gutiérrez et al. described the suitability of poly(vinyl alcohol) scaffolds for 3D culture and resulted in remarkable bacteria accessibility to the whole monolith microstructure (as shown in Fig.

3) [55]. In addition, a macroporous sponge-like scaffold based on partially acetylated dextran (DexAc) monolith was prepared to culture HeLa cells [56]. The result shows that culturing of HeLa cells in the DexAc sponge with fibronectin coating showed that cells distributed homogeneously within the sponge while cells formed clusters in the sponge without coating.

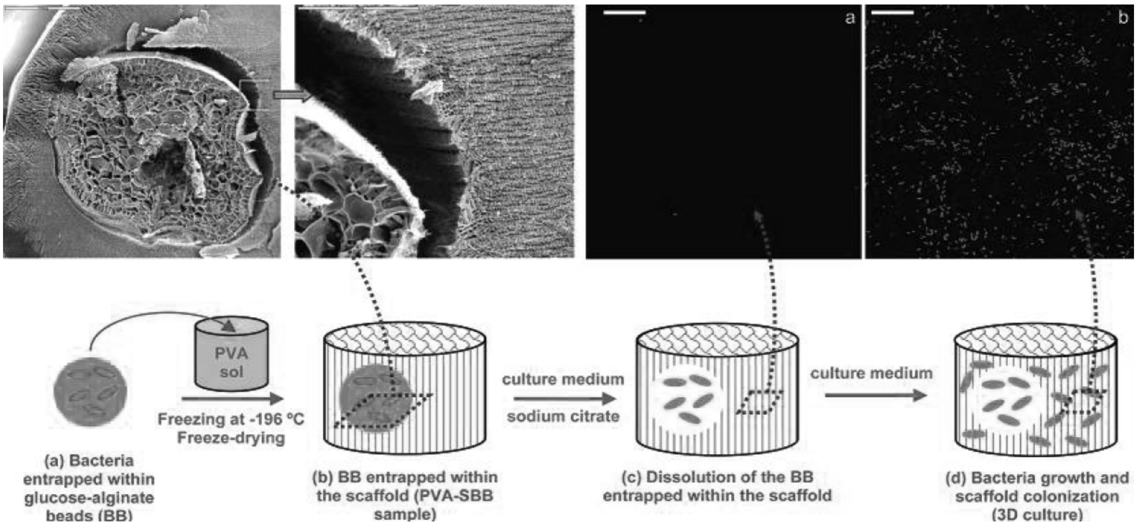

Fig. 3 Poly(vinyl alcohol) (PVA) monolith with 3D structure for bacteria growth [55]

Other applications of monolith, such as controlled drug release, template-assisted synthesis of nanomaterials, adsorption media, immunodiagnostics and even synthetic media in combinatorial chemistry were investigated due to their unique characteristics [57-64].

Currently, there are two main classes of monolithic materials: silica-based monoliths and polymer-based ones. Tanaka et al. first developed silica-based monoliths in the mid-1990s [65-67]. Since then, silica-based monoliths are usually prepared according to a sol-gel process which typically utilizes tetramethoxysilane and tetraethoxysilane as a silica precursor. In addition, additives that induce phase separation include water-soluble polymer and surfactants, for example, poly(ethylene oxide) used as a pore-forming agent. Typical sol-gel reactions responsible to form silica-based monolith is shown in Fig. 4 [68, 69]. A sol is a colloidal suspension which is converted into a gel through polycondensation of the sol forming a wet structure; the gelation process occurs due to the aggregation of polymer particles into fractal clusters, which interpenetrate to some extent and link together forming the network [70].

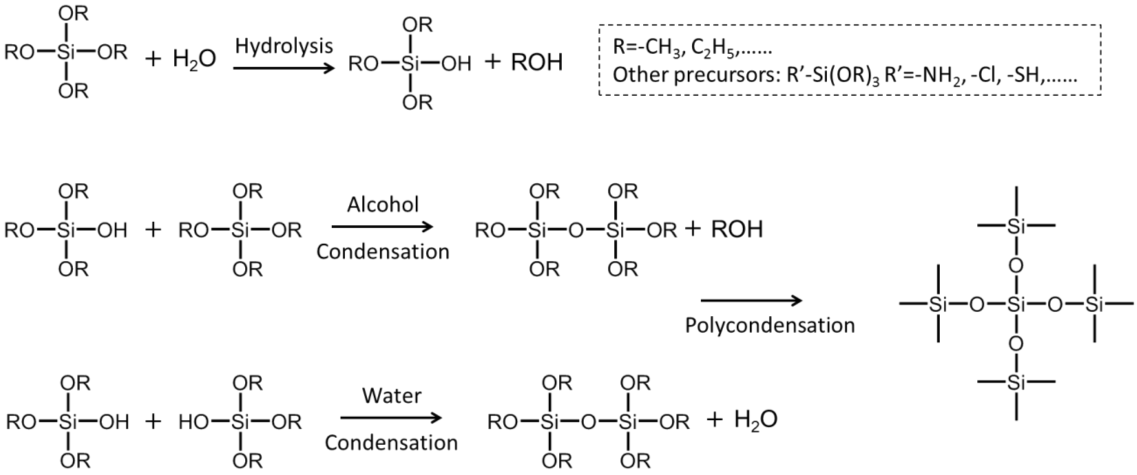

Fig. 4 Typical sol-gel reactions responsible to form silica-based monolith [68,69]

Silica-based monoliths possess an excellent mechanical stability and a high surface area, but their fabrication is challenging because of shrinking of monolithic stationary phase during the gelation process. In order to avoid disintegration of the monolithic stationary phase, the pH has to be limited to a range of 2-8 [71]. Ligands which are entrapped in silica monoliths are also feasible; however, the release of alcohols during the gelation process is not always compatible with labile proteins [72, 73].

Compared to silica-based monoliths, polymer-based monoliths have gradually occupied an impressively critical position because of their good biocompatibility, high mechanical stability and excellent pH stability [74]. Moreover, the polymer monoliths are useful in a wide range of applications since their surface property and functionality can be readily controlled by the proper selection of polymer and the modification [75].

There are various methods to fabricate porous polymer monoliths from the corresponding monomers including polymerization-induced phase separation, polymerization within high internal phase emulsion templates and polycondensation.

Thermally initiated free radical polymerization was the first technique applied for the fabrication of polymer-based monolith [11, 76, 77]. Various numbers of monomers can be used in the fabrication of polymer-based monolith *via* thermally initiated free radical processes. A few examples of monomers used for preparation monolith are shown in Fig. 5 [78].

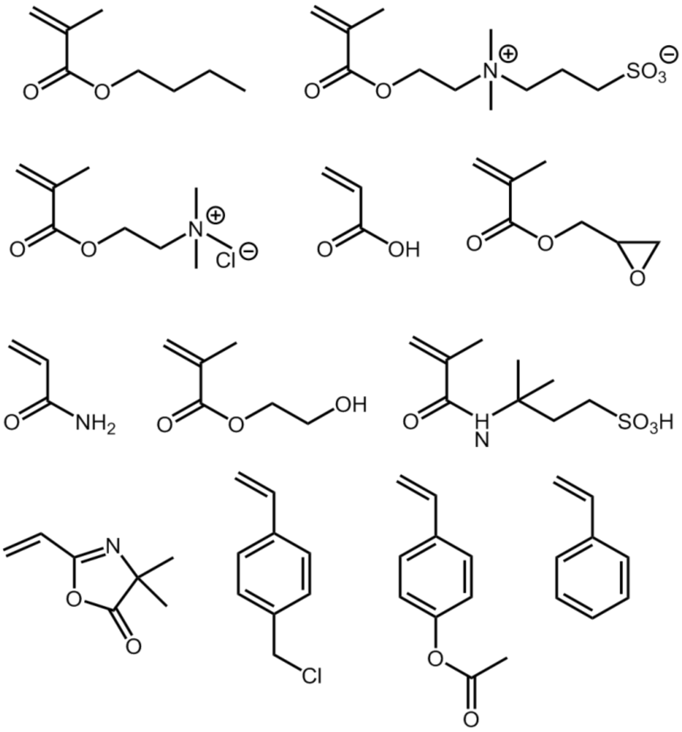

Fig. 5 Examples of monomers applied for fabrication of porous polymer [78]

Preparation of monolith using polymerizations initiated by high energy radiation such as electron beam or γ-ray has a major advantage that the initiator is not required and the polymerization can be carried out at any temperature [79, 80]. During the exposure to ionizing radiation, the ions as well as a large number of free radicals are created to initiate the polymerization, resulting in a crosslinked monolith. In this process, the dose rate is the key factor to control the final porous structure of the monolith. It is reported that under other identical fabrication parameters, the higher dose rate could create more free-radicals to accelerate the polymerization and crosslinking, resulting in larger pore structure. However, a certain drawback is the significant safety requirement while working with radiation.

Another method called polymerized high internal emulsions was first described in detail by Small and Sherrington [81, 82]. They are prepared by emulsifying up to 90% water containing free radical initiator, typically potassium peroxodisulfate, and calcium chloride in 10% of an oil phase comprising monomers such as styrene and divinylbenzene, as well as a surfactant. Upon intensive stirring, this mixture forms a white mass which is then filled in a mold and polymerized at an increase temperature forming a monolith.

Living polymerization is a method in pursuit of better control of porous properties of polymer-based monolith [83, 84]. In this process, the termination and controlled reactions were established by an equilibration between active and dormant species. The polymerization techniques that have attracted attention including atom transfer radical polymerization, nitroxide mediated polymerization, ring-opening metathesis polymerization and reversible addition–fragmentation chain transfer. Some examples of monomers used in the ring-opening metathesis polymerization affording porous materials are shown in Fig. 6 [2].

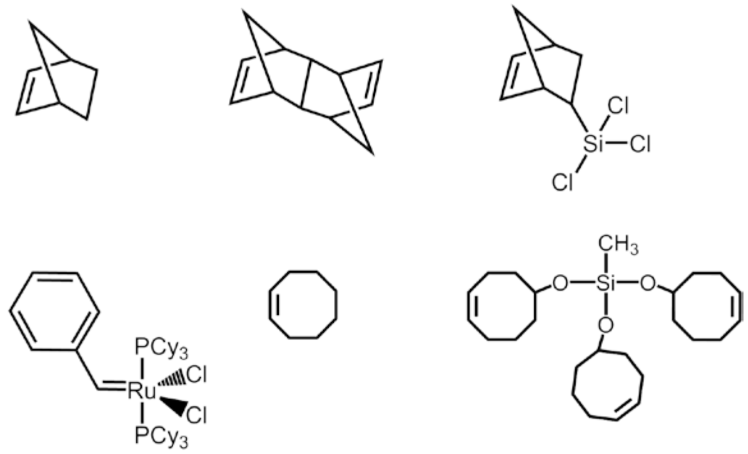

Fig. 6 Examples of monomers used in the ring-opening metathesis polymerization affording porous monoliths [2]

Recently polycondensation became a new contribution to the family of methods enabling the preparation of monolith, which features repeated activation of the chain end thus allowing for growth of all polymer chains in the system no matter how long they are [2]. They are not sensitive to oxygen and the strict de-aeration essential for free radical processes is not needed. Urea-formaldehyde polymer was the first chromatographic monolith prepared by this method [85].

Fig. 7 shows a cryotropic gelation technique that affords spongy hydrophilic monolith called cryogels with large pores, which is a specific type of gel formation that takes place as a result of cryogenic treatment of the systems potentially capable of gelation [86, 87].

However, in most of the polymerization-induced methods, complicated, time-consuming procedures and additives such as porogens are required for the precise morphology control. It is often difficult to obtain the homogeneous porous structure because polymerization and phase separation have to be controlled simultaneously and accurately.

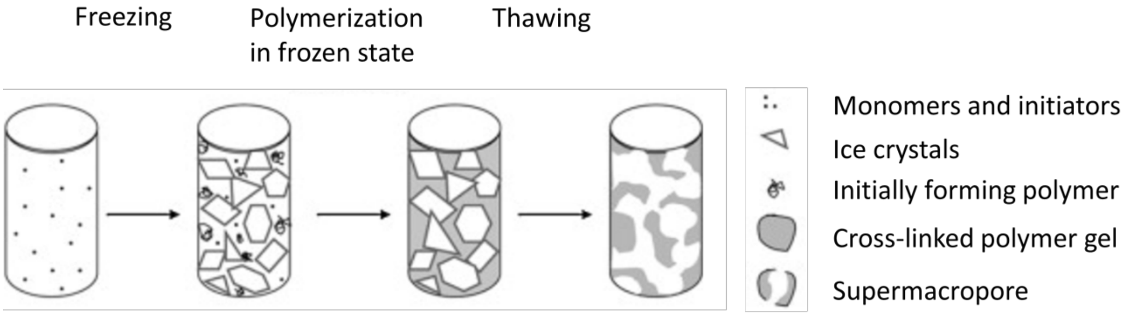

Fig. 7 Scheme of formation of cryogels [86]

Our laboratory have recently developed an easy and straightforward approach to prepare monoliths without any templates, namely thermally induced phase separation (TIPS) technique [88, 89]. The typical procedure of TIPS method is as follows. Polymers are first dissolved in an appropriate solvent by heating, followed by cooling the solution. During the cooling step, the phase separation of the polymer solution takes place to form the monolith with uniform porosity and high surface area without any templates. The shape of the monoliths can be modified by altering the shape of the vessel. In addition, polymer monoliths have been also fabricated by non-solvent induced phase separation (NIPS) [90, 91]. The addition of a non-solvent to a polymer solution induces the phase separation to form a polymer monolith with controlled porous structure.

In contrast with conventional methods to prepare polymer-based monolith, both of TIPS and NIPS method use polymer itself as precursor to prepare monolith without additives, they are simple, fast and time-saving with controlled pore size and distribution. Polyacrylonitrile (PAN) monolith was first published using TIPS method in our lab (Fig. 8) [88]. So far, monoliths of polycarbonate, polyacrylonitrile, poly(vinyl alcohol), poly(γ-glutamic acid) were successfully fabricated in our laboratory [88-93].

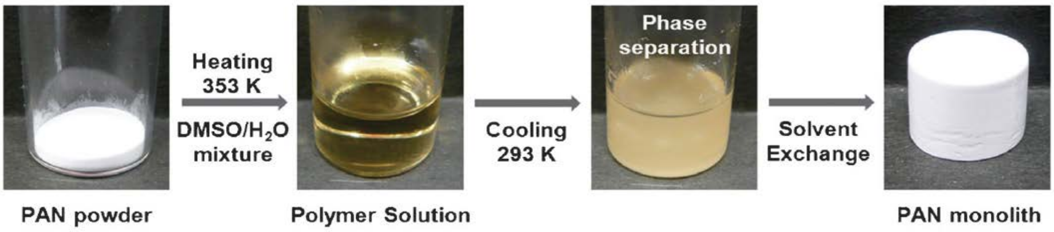

Fig. 8 The protocol for preparation of PAN monolith *via* TIPS method [88]

Nowadays diffident supports are widely used for enzyme immobilization. Enzymes, biocatalysts possessing high specificity and catalytic activity under mild reaction conditions, have been widely used in proteomics and chemical industry due to their chemo-, region- and stereospecificity [94, 95]. One of the drawbacks of enzymes is that they are easily inactivated by external factors like organic solvents, extreme temperature and pH. In addition, it requires a time-consuming and tedious process to separate the enzyme and the product. Therefore, immobilization of enzymes on solid supports has been extensively studied.

So far, various materials have been used to immobilize enzymes [96-99]. The properties of the immobilized enzyme are governed by the properties of both the enzyme and the support material. The interaction between the enzyme and the support could provide the enzyme with specific chemical, biochemical, mechanical and kinetic properties [100]. The support can be a synthetic organic polymer, a biopolymer, or an inorganic solid. It has been demonstrated that chemical compositions as well as morphology of the materials are the critical factors to enhance the catalytic activity, stability and reusability of enzymes. Due to the unique characteristics such as large surface area, excellent permeability, monoliths are suitable for the enzyme immobilization.

There are different methods to prepare immobilized enzyme onto support. Immobilization of an enzyme entails the interaction of two species, the enzyme and the carrier. Some examples are shown in Fig. 9, including adsorption, entrapment, encaplulation, covalent binding [101-103].

The adsorption of enzymes onto supports can proceed *via* different types of interactions. Enzymes with a large lipophilic surface area will interact well with a hydrophobic carrier. Entropy changes and van der Waals forces ensure the immobilization of the enzyme on the support. The advantage of immobilization *via* entropy effects or hydrogen bonds is that the enzyme does not have to be pre-treated or chemically modified [102]. However, a significant disadvantage of immobilizing by adsorption is that the enzyme tends to leach readily from the support when used in aqueous media [104].

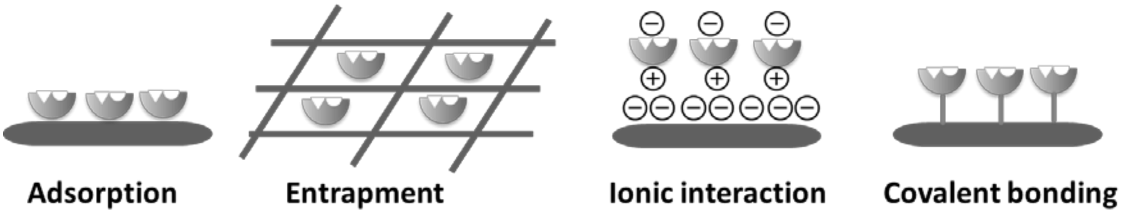

Fig. 9 Different techniques for enzyme immobilization

The efficient means of avoiding any negative influence on the structure of an enzyme is to prepare immobilized enzyme by entrapment. Many methods for entrapment have been developed and the sol-gel method is one of them. Although sol-gels are porous, diffusion of substrate to the enzyme can be restricted [105, 106].

Immobilization *via* ionic interaction is also used [102, 107]. Depending on the pH of the solution and the isoelectric point the surface of the enzyme may bear charges.

Using widely available modelling systems, the surface charge and charge distribution of an enzyme can be readily calculated and displayed [108]. Essentially any ion exchanger can act as support in immobilization *via* ionic and strong polar interactions. Depending on the predominant charge on the enzyme, the ion exchanger needs to be positively charged (for example protonated amino groups) or negatively (for example carboxylate). Ionic immobilization is strongly dependent on the pH value and salt concentrations during immobilization, but also during application. Similar to the leaching in aqueous media described for enzymes immobilized *via* hydrogen bonds, high salt concentrations can lead to ion exchange and washing out of the enzymes immobilized *via* ionic interactions.

Covalent binding of an enzyme to a support has the advantage that the enzyme is tightly fixed [109, 110]. Therefore enzyme leaching in aqueous media is minimized and no enzyme contamination of the product occurs. Generally speaking, covalent immobilization should be prior to other methods when working in aqueous solution and when denaturing factors exist. This is due to the fact that the formation of multiple covalent bonds between the enzyme and the support reduces conformational flexibility and thermal vibrations therefore preventing enzyme unfolding and denaturation. Overall covalently immobilized enzymes can be applied in organic solvent or in pure hydrophobic reactants to avoid leaching.

Table 1 Factors influencing performance of immobilized enzymes

Factors	Implications of immobilization
Hydrophobic partition	Enhancement of reaction rate of hydrophobic substrate
Microenvironment of support	Hydrophobic nature stabilizes enzyme
Multipoint attachment of support	Enhancement of enzyme thermal stability
Spacer or arm of various types of immobilized enzymes	Preventation of enzyme deactivation
Diffusion constraints	Decrease of Enzyme activity and increase of stability
Presence of substrates or inhibitors	Higher activity retention
Physical post-treatments	Improvement of enzyme performance
Different binding mode	Effect on activity and stability
Physical structure of the support such as pore size	Pore-size dependent activity retention
Physical nature of the support	Higher activity retention due to supports with large pore size

The advantages and disadvantages of these methods used for enzyme immobilization are compared above. Furthermore, various factors that influence the performance of immobilized enzyme are summarized in Table 1 [111].

So far, various materials are used for fabrication of immobilization supports, which are divided into three categories, natural polymer, inorganic materials and synthetic polymers [111]. For example, alginate derived from cell walls of brown algae are calcium, magnesium and sodium salts of alginic acid and have been extensively used for immobilization [112]. Chitin and chitosan have also been used as support for immobilization separately or combined with other materials [111, 113]. Other natural polymer, such as collagen, carrageenan, cellulose, starch, and gelatin are also used for immobilization. Inorganic materials such as zeolites, ceramics, celite, silica, glass, activated carbon are also investigated [111, 114].

In addition, there are various polymers that are suitable for preparation of monolith. The characteristics of different polymers are listed in the Table 2. Among these polymers, polymethacrylate materials with high impact resistance, low moisture absorption, biocompatibility, high transparency and low cost are widely applied for contact lenses, bone cement, transparent sheet and car industry [115]. As a result, polymethacrylate-based polymer is a potential material due to the excellent characteristics.

Table 2 Properties and possible applications of polymer-based monoliths fabricated through phase separation method.

Polymers	**Properties**	**Possible Applications**
Acrylic Resin	Chemical Modification Solvent Resistance	Separation Matrix Catalyst Matrix
Poly(acrylonitrile)	Heat Resistance Solvent Resistance	Precursor for Battery Material Separation Matrix
Polyolefin	Heat Resistance Solvent Resistance	Battery Separator Matrix for Fuel Gas
Polycarbonate	Impact Resistance Heat Resistance	Electronic Material Acoustic Material
Poly(vinyl alcohol)	Hydrophilic Solvent Resistance	Biomaterial Separation Matrix
Poly(lactic acid)	Biodegradability Biocompatibility	Agriculture Material Biomaterial
Polyurethane	Flexibility Absorbability	Acoustic Material Cosmetic
Poly(γ- glutamic acid)	Hydrophilic Biocompatibility	Biomaterial Cosmetic
Silk	Hydrophilic Biocompatibility	Biomaterial Cosmetic
Cellulose	Hydrophilic Solvent Resistance	Biomaterial Catalyst Matrix

Based on the background mentioned above, a reactive poly(glycidyl methacrylate-*co*-methyl methacrylate) (PGM) with epoxy group as shown in Fig. 10 will be used to prepare polymer-based monolith in a facile method. This thesis is composed of three chapters concerning the fabrication of PGM monoliths *via* TIPS method and their applications for covalent immobilization of enzyme.

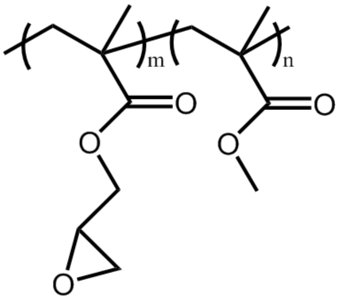

Fig. 10 Chemical structure of PGM

In Chapter 1, PGM copolymer is synthesized from glycidyl methacrylate and methyl methacrylate through conventional radical polymerization and PGM monoliths with three-dimensional continuous interconnected porous structure in a single piece are prepared *via* TIPS method for the first time. The morphology of the PGM monolith is observed through SEM. The effects of the fabrication parameters such as polymer concentration and cooling temperature on the skeleton and pore sizes of the PGM monolith are discussed. The mechanism of forming PGM monolith is discussed and the hypothesis of the effect of the parameters on the pore structure is proposed.

In Chapter 2, horseradish peroxidase (HRP), a widely used oxidase enzyme, is selected as a model enzyme to investigate the monolith as an immobilizing support. This chapter describes immobilization of HRP onto a modified PGM monolith. The PGM monolith is modified with adipic acid dihydrazide (AADH) and ethylenediaminetetraacetic dianhydride (EDTAD) to yield carboxyl group-bearing PGM (PGM-COOH) monolith. The PGM-COOH monolith is reacted with *N*-hydroxysuccineimide (NHS) to activate the carboxyl groups on the monolith and further modified with HRP. The activity and reusability of the immobilized HRP are discussed. Furthermore, three kinds of diamine reagents with spacer having different length are used to investigate the effect of the interference on the modification of PGM monolith and immobilization of HRP. Moreover, the immobilized HRP on immobilized PGM monolith with different spacer lengths are applied for phenol removal.

In Chapter 3, a PGM monolith prepared *via* TIPS method is used as a solid support to covalently immobilize pepsin which is a widely used proteolytic enzyme. The PGM monolith is modified with aminoacetal to yield an aldehyde-bearing (PGM-CHO) monolith. Pepsin is immobilized onto the PGM-CHO monolith *via* reductive amination. The activity of the free and immobilized pepsin is investigated. Furthermore, the PGM-CHO monolith modified with pepsin is applied for online protein digestion followed by LC-MS and LC-MS/MS analyses. The efficiency and the reproducibility of the pepsin column are discussed.

References

[1]. Svec F and Frechet JM. *Science*. 1996;273(5272):205-211.

[2]. Svec F. *Journal of Chromatography A*. 2010;1217(6):902-924.

[3]. Rhodes KH, Davis SA, Caruso F, Zhang B, and Mann S. *Chemistry of Materials*. 2000;12(10):2832-2834.

[4]. Hoffmann F, Cornelius M, Morell J, and Fröba M. *Angewandte Chemie*

International Edition. 2006;45(20):3216-3251.

[5]. Namera A, Nakamoto A, Saito T, and Miyazaki S. *Journal of Separation Science*. 2011;34(8):901-924.

[6]. Svec F and Fréchet JM. *Analytical Chemistry*. 1992;64(7):820-822.

[7]. Mould D and Synge R. *Analyst*. 1952;77(921):964-969.

[8]. Ross WD and Jefferson RT. *Journal of Chromatographic Science*. 1970;8(7):386-389.

[9]. Schnecko H and Bieber O. *Chromatographia*. 1971;4(3):109-112.

[10]. Hileman F, Sievers R, Hess G, and Ross W. *Analytical Chemistry*. 1973;45(7):1126-1130.

[11]. Hjerten S, Liao J-L, and Zhang R. *Journal of Chromatography A*. 1989;473:273-275.

[12]. Gritti F and Guiochon G. *Journal of Chromatography A*. 2012;1228:2-19.

[13]. Lau CH, Li P, Li F, Chung T-S, and Paul DR. *Progress in Polymer Science*. 2013;38(5):740-766.

[14]. Ambashta RD and Sillanpää ME. *Journal of Environmental Radioactivity*. 2012;105:76-84.

[15]. Wang QC, Svec F, and Frechet JM. *Analytical Chemistry*. 1993;65(17):2243-2248.

[16]. Svec F and Huber CG. *Analytical Chemistry*. 2006;78(7):2100-2107.

[17]. Unger KK, Skudas R, and Schulte MM. *Journal of Chromatography A*. 2008;1184(1):393-415.

[18]. Ghanem A and Ikegami T. *Journal of Separation Science*. 2011;34(16‐17):1945-1957.

[19]. Iberer G, Hahn R, and Jungbauer A. *LC GC*. 1999;17(11):998-1005.

[20]. Svec F. *LC GC EUROPE*. 2003;16(6 A):24-28.

[21]. Jungbauer A and Hahn R. *Journal of Chromatography A*. 2008;1184(1):62-79.

[22]. Luedtke S, Adam T, Von Doehren N, and Unger K. *Journal of Chromatography A*. 2000;887(1):339-346.

[23]. Colón LA, Maloney TD, and Fermier AM. *Journal of Chromatography A*. 2000;887(1):43-53.

[24]. Guo W, Yang C, and Xu B. *Journal of Chromatography A*. 2004;1059(1):175-180.

[25]. Bujalski R and Cantwell FF. *Journal of Chromatography A*. 2004;1048(2):173-181.

[26]. Nguyen DTT, Guillarme D, Rudaz S, and Veuthey JL. *Journal of Separation Science*. 2006;29(12):1836-1848.

[27]. Lubbad S, Mayr B, Huber CG, and Buchmeiser MR. *Journal of Chromatography A*. 2002;959(1):121-129.

[28]. Josic D, Buchacher A, and Jungbauer A. *Journal of Chromatography B: Biomedical Sciences and Applications*. 2001;752(2):191-205.

[29]. Jungbauer A. *Journal of Chromatography A*. 2005;1065(1):3-12.

[30]. Mayr B, Tessadri R, Post E, and Buchmeiser MR. *Analytical Chemistry*. 2001;73(17):4071-4078.

[31]. Peters EC, Svec F, and Fréchet J. *Advanced Materials*. 1999;11(14):1169-1181.

[32]. Nischang I, Teasdale I, and Brüggemann O. *Analytical & Bioanalytical Chemistry*. 2011;400(8):2289-2304.

[33]. Svec F. *Journal of Separation Science*. 2004;27(10‐11):747-766.

[34]. Le Gac S, Carlier J, Camart J-C, Cren-Olivé C, and Rolando C. *Journal of Chromatography B*. 2004;808(1):3-14.

[35]. Moore RE, Licklider L, Schumann D, and Lee TD. *Analytical Chemistry*. 1998;70(23):4879-4884.

[36]. Svec F, Peters EC, Sykora D, Yu C, and Frechet J. *Journal of High Resolution Chromatography*. 2000;23(1):3-18.

[37]. Stachowiak TB, Svec F, and Fréchet JM. *Journal of Chromatography A*. 2004;1044(1):97-111.

[38]. Svec F. *Journal of Chromatography B*. 2006;841(1):52-64.

[39]. Bakry R, Bonn GK, Mair D, and Svec F. *Analytical Chemistry*. 2007;79(2):486-493.

[40]. Anderson EB and Buchmeiser MR. *ChemCatChem*. 2012;4(1):30-44.

[41]. Buchmeiser MR. *Chemical Reviews*. 2008;109(2):303-321.

[42]. Nandi M and Uyama H. *RSC Advances*. 2014;4(40):20847-20855.

[43]. Burguete MI, García-Verdugo E, Karbass N, Luis SV, Sans V, and Sokolova M. *Pure & Applied Chemistry*. 2009;81(11):1991-2000.

[44]. Frost CG and Mutton L. *Green Chemistry*. 2010;12(10):1687-1703.

[45]. Dräger G, Kiss C, Kunz U, and Kirschning A. *Organic & Biomolecular Chemistry*. 2007;5(22):3657-3664.

[46]. Mayr M, Mayr B, and Buchmeiser MR. *Angewandte Chemie International Edition*. 2001;40(20):3839-3842.

[47]. Xie S, Svec F, and Fréchet JM. *Biotechnology & Bioengineering*. 1999;62(1):30-35.

[48]. Tsujioka N, Hira N, Aoki S, Tanaka N, and Hosoya K. *Macromolecules*.

2005;38(24):9901-9903.

[49]. Mayr M, Wang D, Kröll R, Schuler N, Prühs S, Fürstner A, and Buchmeiser MR. *Advanced Synthesis & Catalysis*. 2005;347(2-3):484-492.

[50]. Hayward AS, Eissa AM, Maltman DJ, Sano N, Przyborski SA, and Cameron NR. *Biomacromolecules*. 2013;14(12):4271-4277.

[51]. Christenson EM, Soofi W, Holm JL, Cameron NR, and Mikos AG. *Biomacromolecules*. 2007;8(12):3806-3814.

[52]. Yamada KM and Cukierman E. *Cell*. 2007;130(4):601-610.

[53]. Pampaloni F, Reynaud EG, and Stelzer EH. *Nature Reviews Molecular Cell Biology*. 2007;8(10):839-845.

[54]. Kircher L, Theato P, and Cameron NR. *Polymer*. 2013;54(7):1755-1761.

[55]. Gutiérrez MC, García-Carvajal ZY, Jobbágy M, Yuste L, Rojo F, Abrusci C, Catalina F, del Monte F, and Ferrer ML. *Chemistry of Materials*. 2007;19(8):1968-1973.

[56]. van der Vlies AJ, Han W, Uyama H, and Hasegawa U. *Journal of Biomaterials and Tissue Engineering*. 2014;4(1):28-36.

[57]. Wu Q, Bienvenue JM, Hassan BJ, Kwok YC, Giordano BC, Norris PM, Landers JP, and Ferrance JP. *Analytical Chemistry*. 2006;78(16):5704-5710.

[58]. Minaberry Y, Chiappetta DA, Sosnik A, and Jobbágy M. *Biomacromolecules*. 2012;14(1):1-9.

[59]. Grant NC, Cooper AI, and Zhang H. *ACS Applied Materials and Interfaces*. 2010;2(5):1400-1406.

[60]. Gatschelhofer C, Prasch A, Buchmeiser MR, Zimmer A, Wernig K, Griesbacher M, Pieber TR, and Sinner FM. *Analytical Chemistry*. 2012;84(17):7415-7421.

[61]. Ren L-H, Zhang H-L, Lu A-H, Hao Y, and Li W-C. *Microporous & Mesoporous Materials*. 2012;158:7-12.

[62]. Toberer ES, Joshi A, and Seshadri R. *Chemistry of Materials*. 2005;17(8):2142-2147.

[63]. Marco-Lozar J, Kunowsky M, Suárez-García F, Carruthers J, and Linares-Solano A. *Energy & Environmental Science*. 2012;5(12):9833-9842.

[64]. Sá J, Fernandes DLA, Aiouache F, Goguet A, Hardacre C, Lundie D, Naeem W, Partridge WP, and Stere C. *Analyst*. 2010;135(9):2260-2272.

[65]. Minakuchi H, Nakanishi K, Soga N, Ishizuka N, and Tanaka N. *Analytical Chemistry*. 1996;68(19):3498-3501.

[66]. Ishizuka N, Minakuchi H, Nakanishi K, Soga N, Hosoya K, and Tanaka N. *Journal of High Resolution Chromatography*. 1998;21(8):477-479.

[67]. Tanaka N, Kobayashi H, Ishizuka N, Minakuchi H, Nakanishi K, Hosoya K, and Ikegami T. *Journal of Chromatography A*. 2002;965(1):35-49.

[68]. Kato M, Sakai‐Kato K, and Toyo'oka T. *Journal of Separation Science*. 2005;28(15):1893-1908.

[69]. Szumski M and Buszewski B. *Journal of Separation Science*. 2007;30(1):55-66.

[70]. Siouffi A-M. *Journal of Chromatography A*. 2003;1000(1):801-818.

[71]. Ahmed A, Clowes R, Myers P, and Zhang H. *Journal of Materials Chemistry*. 2011;21(15):5753-5763.

[72]. Jin W and Brennan JD. *Analytica Chimica Acta*. 2002;461(1):1-36.

[73]. Sakai-Kato K, Kato M, and Toyo'oka T. *Analytical Chemistry*. 2002;74(13):2943-2949.

[74]. Nordborg A and Hilder EF. *Analytical & Bioanalytical Chemistry*.

2009;394(1):71-84.

[75]. Gillespie E, Connolly D, and Paull B. *Analyst*. 2009;134(7):1314-1321.

[76]. Tennikova T, Svec F, and Belenkii B. *Journal of Liquid Chromatography*. 1990;13(1):63-70.

[77]. Tennikova T, Bleha M, Švec F, Almazova T, and Belenkii B. *Journal of Chromatography A*. 1991;555(1):97-107.

[78]. Wang QC, Švec F, and Fréchet JM. *Journal of Chromatography A*. 1994;669(1):230-235.

[79]. Viklund C and Irgum K. *Macromolecules*. 2000;33(7):2539-2544.

[80]. Gu B, Li Y, and Lee ML. *Analytical Chemistry*. 2007;79(15):5848-5855.

[81]. Small PW and Sherrington DC. *Journal of the Chemical Society, Chemical Communications*. 1989(21):1589-1591.

[82]. Hainey P, Huxham I, Rowatt B, Sherrington D, and Tetley L. *Macromolecules*. 1991;24(1):117-121.

[83]. Georges MK, Veregin RP, Kazmaier PM, and Hamer GK. *Macromolecules*. 1993;26(11):2987-2988.

[84]. Saban MD, Georges MK, Veregin RP, Hamer GK, and Kazmaier PM. *Macromolecules*. 1995;28(20):7032-7034.

[85]. Sun X and Chai Z. *Journal of Chromatography A*. 2002;943(2):209-218.

[86]. Plieva FM, Galaev IY, and Mattiasson B. *Journal of Separation Science*. 2007;30(11):1657-1671.

[87]. Plieva FM, Savina IN, Deraz S, Andersson J, Galaev IY, and Mattiasson B. *Journal of Chromatography B*. 2004;807(1):129-137.

[88]. Okada K, Nandi M, Maruyama J, Oka T, Tsujimoto T, Kondoh K, and Uyama H.

Chemical Communications. 2011;47(26):7422-7424.

[89]. Nandi M, Okada K, and Uyama H. *Functional Materials Letters*. 2011;4(04):407-410.

[90]. Xin Y and Uyama H. *Chemistry Letters*. 2012;41(11):1509-1511.

[91]. Xin Y, Fujimoto T, and Uyama H. *Polymer*. 2012;53(14):2847-2853.

[92]. Sun X and Uyama H. *Nanoscale Research Letters*. 2013;8(1):1-5.

[93]. Park S-B, Sakamoto J, Sung M-H, and Uyama H. *Polymer*. 2013;54(22):6114-6118.

[94]. Schoemaker HE, Mink D, and Wubbolts MG. *Science*. 2003;299(5613):1694-1697.

[95]. Schmid A, Dordick J, Hauer B, Kiener A, Wubbolts M, and Witholt B. *Nature*. 2001;409(6817):258-268.

[96]. Chen B, Pernodet N, Rafailovich MH, Bakhtina A, and Gross RA. *Langmuir*. 2008;24(23):13457-13464.

[97]. Zhang J, Zhang F, Yang H, Huang X, Liu H, Zhang J, and Guo S. *Langmuir*. 2010;26(9):6083-6085.

[98]. Juang R-S, Wu F-C, and Tseng R-L. *Bioresource Technology*. 2001;80(3):187-193.

[99]. DeLouise LA and Miller BL. *Analytical Chemistry*. 2005;77(7):1950-1956.

[100]. Sheldon RA and van Pelt S. *Chemical Society Reviews*. 2013;42(15):6223-6235.

[101]. Mateo C, Palomo JM, Fernandez-Lorente G, Guisan JM, and Fernandez-Lafuente R. *Enzyme & Microbial Technology*. 2007;40(6):1451-1463.

[102]. Cao L. Carrier-bound immobilized enzymes: principles, application and design.

John Wiley & Sons, 2006.

[103]. Sheldon RA. *Advanced Synthesis & Catalysis*. 2007;349(8‐9):1289-1307.

[104]. Ferrer M, Plou FJ, Fuentes G, Cruces MA, Andersen L, Kirk O, Christensen M, and Ballesteros A. *Biocatalysis & Biotransformation*. 2002;20(1):63-71.

[105]. Pierre A. *Biocatalysis & Biotransformation*. 2004;22(3):145-170.

[106]. Ge X, Eleftheriou NM, Dahoumane SA, and Brennan JD. *Analytical Chemistry*. 2013;85(24):12108-12117.

[107]. Yiu HH and Wright PA. *Journal of Materials Chemistry*. 2005;15(35-36):3690-3700.

[108]. Basso A, Maltman BA, Flitsch SL, Margetts G, Brazendale I, Ebert C, Linda P, Verdelli S, and Gardossi L. *Tetrahedron*. 2005;61(4):971-976.

[109]. Basso A, Braiuca P, Cantone S, Ebert C, Linda P, Spizzo P, Caimi P, Hanefeld U, Degrassi G, and Gardossi L. *Advanced Synthesis & Catalysis*. 2007;349(6):877-886.

[110]. Boller T, Meier C, and Menzler S. *Organic Process Research & Development*. 2002;6(4):509-519.

[111]. Datta S, Christena LR, and Rajaram YRS. *3 Biotech*. 2013;3(1):1-9.

[112]. Flores-Maltos A, Rodríguez-Durán LV, Renovato J, Contreras JC, Rodríguez R, and Aguilar CN. *Enzyme Research*. 2011;2011.

[113]. Chang M-Y and Juang R-S. *Biochemical Engineering Journal*. 2007;35(1):93-98.

[114]. Chang Y-K and Chu L. *Biochemical Engineering Journal*. 2007;35(1):37-47.

[115]. Tsai T-L, Lin C-C, Guo G-L, and Chu T-C. *Industrial & Engineering Chemistry Research*. 2008;47(8):2554-2560.

Chapter 1

Fabrication and Characterization of PGM Monolith *via* Thermally Induced Phase Separation

1.1 Introduction

In general, “monolith" means "one piece". In the field of materials science and engineering, a monolith is often regarded as a single-piece bulk material having three-dimensionally developed continuous pores [1, 2]. Such a monolithic structure is featured by several key aspects such as large surface area, high stability, efficient mass transfer, and high mechanical strength [3-5].These aspects are attractive for its practical use in chromatography, ion-exchange and catalysis and other applications [6-11]. In addition, they can be further upvalued by purpose-designing of the porosity and/or various chemical modifications [12-14].

Currently, there are two main classes of monolithic materials: silica-based and polymer-based monoliths. Silica-based monoliths have serious defects in their industrial applications such as limited pH stability, complicated and sensitive operating protocols, whereas polymer-based monoliths have attracted great interests because of their good biocompatibility, high mechanical stability and excellent pH stability [15]. Moreover, the polymer monoliths are useful in a wide range of applications since their surface property and functionality can be controlled by the proper selection of polymers and their modification [16].

There are many methods to fabricate porous polymer monoliths from the corresponding monomers including polymerization-induced phase separation, polymerization within high internal phase emulsion templates and cryogelation [17-24]. In most of the reported methods, however, complicated, time-consuming procedures and additives such as porogens are required for the precise morphology control; it is often difficult to obtain the homogeneous porous structure because polymerization and phase separation have to be controlled simultaneously and accurately.

Recently, in our lab an easy and straightforward approach is developed to prepare a polymer-based monolith by using a thermally induced phase separation (TIPS) technique which is a template-free method [25, 26]. Polymers are first dissolved in an appropriate solvent by heating, followed by cooling the solution. During the cooling step, the phase separation of the polymer solution takes place to form the monolith with uniform porosity and high surface area without any templates. The shape of the monoliths can be modified by altering the shape of the vessel. Furthermore, polymer monoliths have been also fabricated by non-solvent induced phase separation (NIPS) [27, 28]. The addition of a non-solvent to a polymer solution induces the phase separation to form a polymer monolith with controlled porous structure. So far, monoliths of polycarbonate, polyacrylonitrile, poly(vinyl alcohol), and poly(γ-glutamic acid) have been successfully fabricated [25-33].

In this chapter, fabrication of a poly(glycidyl methacrylate-*co*-methyl methacrylate) (PGM) monolith by TIPS is demonstrated. Ethanol and water are well known as non-solvent of PGM. In our previous reports on fabrication of monoliths by TIPS or NIPS, a mixture of solvent and non-solvent is used for the phase separation, meaning that the solubility of the polymer should be precisely tuned by the mixed ratio of solvent and non-solvent. Interestingly, we find that PGM could be solubilized at 60

^{o}C in a mixture of water and ethanol, both of which are non-solvents for PGM, and the monolith is formed upon cooling. The effect of preparation parameters such as polymer concentration and cooling temperature will be discussed. The surface area of the monolith obtained at different conditions will be compared. In addition, the mechanism of forming monolith will be proposed.

1.2 Experimental

Material

The monomers, methyl methacrylate (MMA) and glycidyl methacrylate (GMA) are purchased from Nacalai Tesque. Azobisisobutyronitrile (AIBN) as an initiator is recrystallized before polymerization. Toluene as a reaction medium is purchased from Wako Pure Chemical Industries Ltd. and dehydrated by molecular sieve. Methanol and ethanol are used as received from Wako Pure Chemical Industries Ltd without further purification.

Instrumentation

Scanning electron microscopic (SEM) images were recorded on a Hitachi SU3500 instrument (Tokyo, Japan) at an accelerating voltage of 15 kV. A thin gold film was sputtered on the samples before the images were collected. Nitrogen adsorption/desorption isotherms were measured with a NOVA 4200e surface area & pore size analyzer (Quantachrome Instruments) at 25 ^{o}C. The specific surface area of the sample was calculated by the Brunauer-Emmett-Teller (BET) method at the linear part of the adsorption branch. Before the measurements, all samples were degassed at 25 ^{o}C for at least 6 h under vacuum. ^{1}H NMR spectra were recorded on a Bruker DPX-400 instrument by using $CDCl_3$ as a solvent. Size exclusion chromatography analysis was carried out using a TOSOH SC8020 apparatus with an RI detector at 40 °C under the following conditions: TOSOH TSKgel G3000H_{HR} column and chloroform eluent at a flow rate of 1.0 mL/min. The calibration curve was obtained using polystyrene standards.

Synthesis of poly (methyl methacrylate-co-glycidyl methacrylate) (PGM)

GMA (4.16 g, 32 mM), MMA (30 g, 300mM) and AIBN (30 mg, 0.13 mM) were dissolved in an excess of solvent (100 mL toluene). After the gently stirring under Ar gas bubbling for 15 min, the mixture was then brought to 80 ^{o}C for 4 hours with stirring to complete the polymerization. After the required time, the reaction mixture was poured into access methanol. The precipitate was filtered and dried in vacuum to get the copolymer as white solid. The polymerization is shown in Fig.1-1.

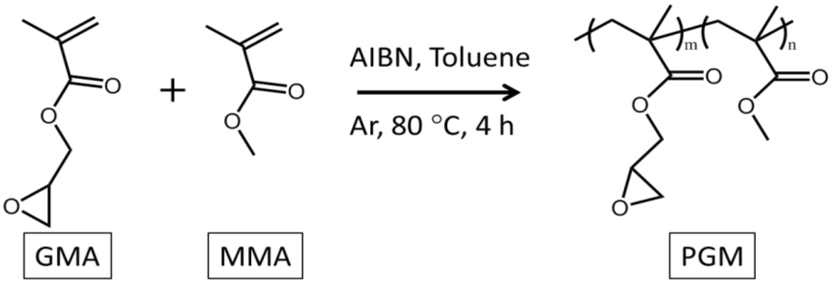

Fig. 1-1 Synthesis of PGM copolymer

Preparation of PGM monolith

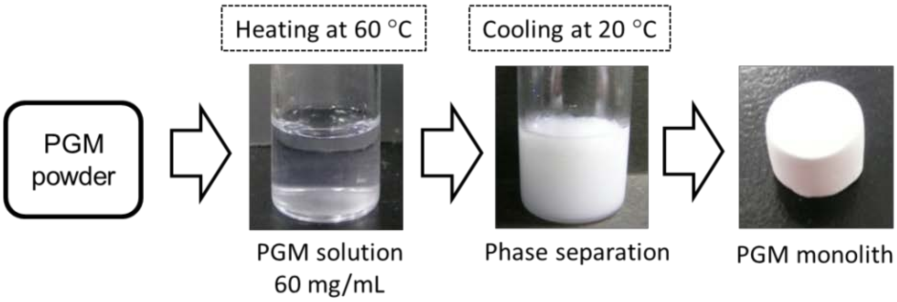

Fig. 1-2 Typical procedure of preparation of PGM monolith

The PGM monolith was prepared *via* TIPS method as shown in Fig. 1-2. A typical procedure is as follows: 90 mg PGM powder was dissolved in 1.5 mL mixture of ethanol/water (80/20 v/v) at 60 °C, and the homogenous solution was cooled down to 20 °C to induce phase separation. The PGM monolith was obtained as a white solid. This monolith was washed with deionized water to remove ethanol and dried in vacuum.

Effect of cooling temperature on pore structure

Different cooling temperatures were used to investigate the effects on pore structure of PGM monolith. The morphology of monolith at three different cooling temperatures, -196, 0 and 20 °C, were compared. Other conditions are shown as follows: the polymer concentration at 60 mg/mL, the heating temperature at 60 °C and the ratio of ethanol/H_2O at 80/20 (v/v).The skeleton and pore sizes were measured under the help of the software Image-Pro Plus.

Effect of polymer concentration on pore structure

Different polymer concentrations were used to investigate the effects on pore structure of PGM monolith. The morphology of monolith at three different polymer concentrations, 40, 60, 80 and 100 mg/mL, were compared. Other conditions are shown as follows: the heating temperature at 60 °C, the cooling temperature at 20 °C and the ratio of ethanol/H_2O at 80/20 (v/v).

1.3 Results and Discussion

Synthesis of PGM copolymer

PGM was synthesized by a conventional radical copolymerization of GMA and MMA with the GMA content of 10 mol%. After copolymerization, 14.4 g white solid polymer is obtained, which indicates that the yield of this reaction is 42%. The molecular weight of M_n is 1.4×10^5 determined by SEC analysis. ^{1}H NMR spectrum of PGM in $CDCl_3$ is shown in Fig. 1-3. ^{1}H NMR (400 MHz, $CDCl_3$) δ=2.6-3.4(3H, oxirane CH) 3.6 (25H, methoxyl CH). The unit ratio of MMA and GMA determined by ^{1}H NMR spectroscopy was 89/11.

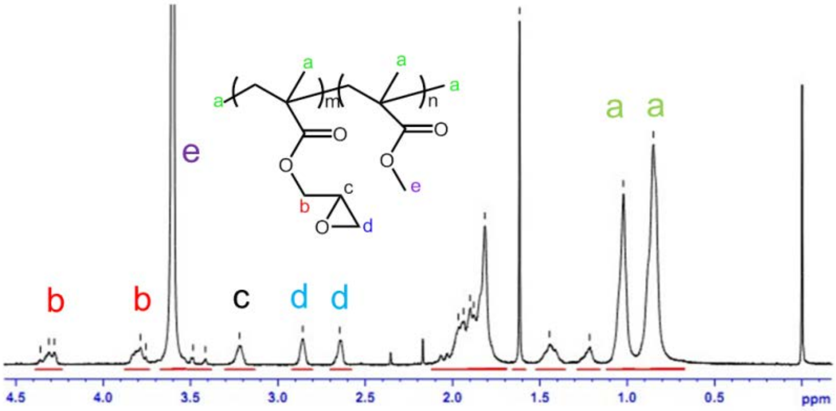

Fig. 1-3 ^{1}H NMR spectra of PGM polymer in $CDCl_3$

Fabrication of PGM monolith

Water and ethanol are well known as non-solvent for PGM. These solvents are more hydrophilic than PGM. Thus, such a mixed solvent, in general, would not solubilize PGM. Actually, PGM was not soluble in a mixture of ethanol and water (80/20 v/v) at room temperature, but we found that it became soluble in this solvent at 60 ^{o}C at the concentration of 40 mg/mL, which may be explained by the unique cosolvency of such a mixed solvent for PGM [34]; the cosolvency effect is that binary solvent mixtures of which both do not solubilize a polymer, but when they are used together in a homogeneous mixture, they create a powerful polymer dissolving system [34]. Furthermore, the phase separation of the PGM solution took place upon cooling to form the uniform monolithic material. The cross-sectional image of the isolated monolith showed the homogeneous three-dimensional interconnected porous structure (Fig. 1-4).

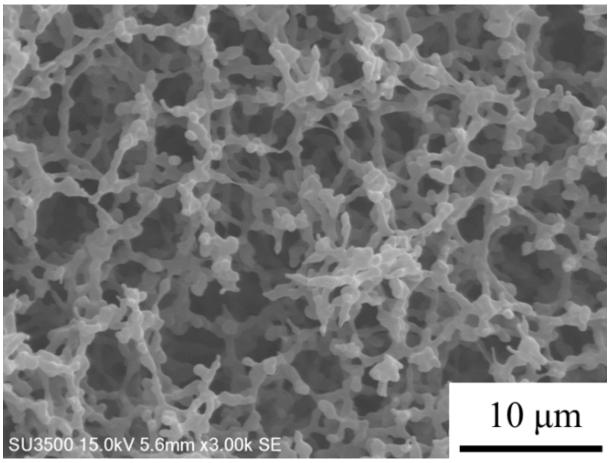

Fig. 1-4 SEM image of PGM monolith (concentration 60 mg/mL, cooling temperature 20 °C)

Characterization

The adsorption of guest molecules onto the solid surface plays an essential role in determining the properties of porous compounds. This adsorption is governed not only by the interaction between guest molecules and the surfaces but also by the pore size and shape. Pores are classified according to their size as follows: ultramicropores (<0.5 nm), micropores (0.5-2 nm), mesopores (2-50 nm) and macropores(>50 nm) [35]. There are six representative adsorption isotherms that reflect the relationship between porous structure and sorption type, which was classified by IUPAC [36]. The adsorption by a macropore can be well explained by the Brunauer-Emmett-Teller (BET) equation [37]. Based on the information mentioned above, the adsorption/desorption isotherms of the PGM monolith at 77K is shown in Fig. 1-5, which could be assigned to a type Ⅲ adsorption with H3 type hysteresis loop in the P/P_0 range from 0 to 1, characteristic of macroporous solid surface and unrestricted monolayer-multilayer adsorption. The specific surface area was determined to be 4.2 m^2/g considering monolayer adsorption by using BET method. This result indicated the large macropore of the PGM monolith.

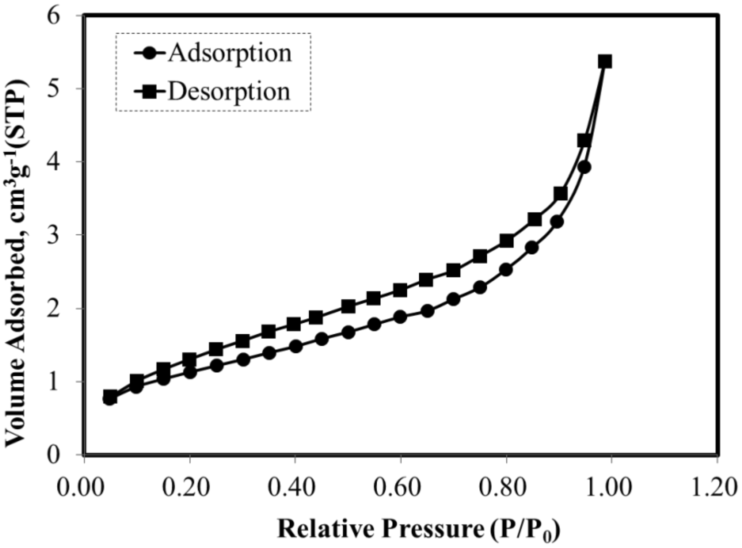

Fig.1-5 Nitrogen adsorption/desorption isotherms of PGM monolith

Effect of cooling temperature

Table 1-1 The surface area of PGM monolith at different cooling temperatures

Cooling temperature (°C)	-196	0	20
Surface area (m^2/g)	15.3	12.4	4.2

The preparation conditions were investigated including cooling temperature and polymer concentration in order to control the morphology precisely. The effect of cooling temperature on the PGM monolith structure was evaluated at -196, 0, 20 °C. The surface areas of monolith obtained at different cooling temperatures were compared. The result is shown in Table 1-1. As we can see, the surface area decreased as the cooling temperature increased. The morphology of PGM monolith observed by SEM and size of the pore structure obtained by the software are shown in Fig. 1-6. The average pore size of the monolith obtained at 20 °C was 4.5 ± 0.7 μm which is larger than that at -196 °C (1.7 ± 0.3 μm). The skeleton size showed a similar trend. These results indicate that the lower cooling temperature provides monoliths with smaller skeleton and pore sizes. Importantly, the significant differences of the pore and skeleton sizes indicate that the cooling temperature plays an important role in controlling the morphology of the PGM monolith.

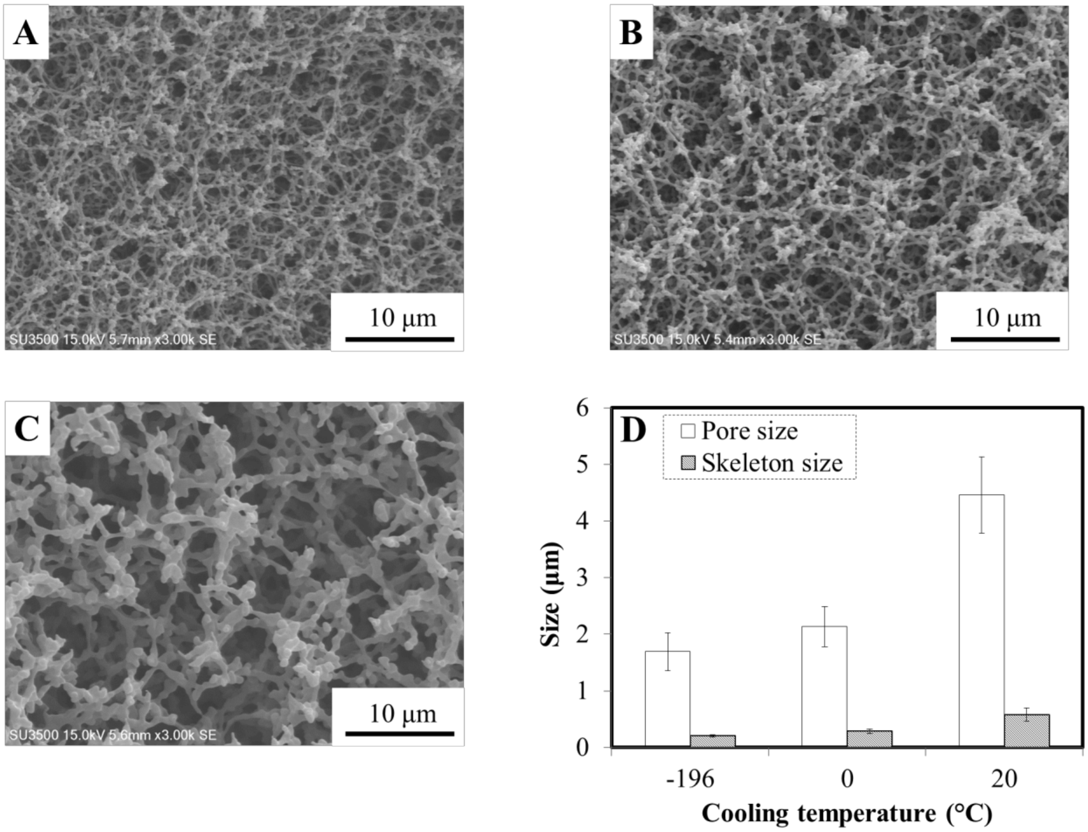

Fig. 1-6 SEM images showing the effect of the cooling temperature on the morphology of the PGM monolith (A) -196 °C, (B) 0 °C, (C) 20 °C (D) The pore and skeleton sizes of PGM monolith at different cooling temperatures.

Effect of polymer concentration

The effect of polymer concentration on the PGM monolith structure was evaluated at 40, 60, 100 mg/mL. The surface areas of monolith obtained at different polymer concentrations were compared. The result is shown in Table 1-2. As we can see, the surface area increased as the polymer concentration increased. Fig. 1-7 represents SEM micrographs showing the influence of the polymer concentration on the morphology of the PGM monolith. As the polymer concentration increased from 40 to 100 mg/mL, the average pore size decreased from 5.6 ± 0.9 to 2.3 ± 0.6 μm and the skeleton size decreased from 0.9 ± 0.1 to 0.3 ± 0.1 μm. These data showed that the polymer concentration significantly affected the pore structure of the PGM monolith, that is, the higher polymer concentration resulted in the formation of a monolith with smaller pore and skeleton sizes.

Table 1-2 The surface area of PGM monolith at different polymer concentration

Polymer concentration(mg/mL)	40	60	100
Surface area (m^2/g)	3.5	4.2	6.9

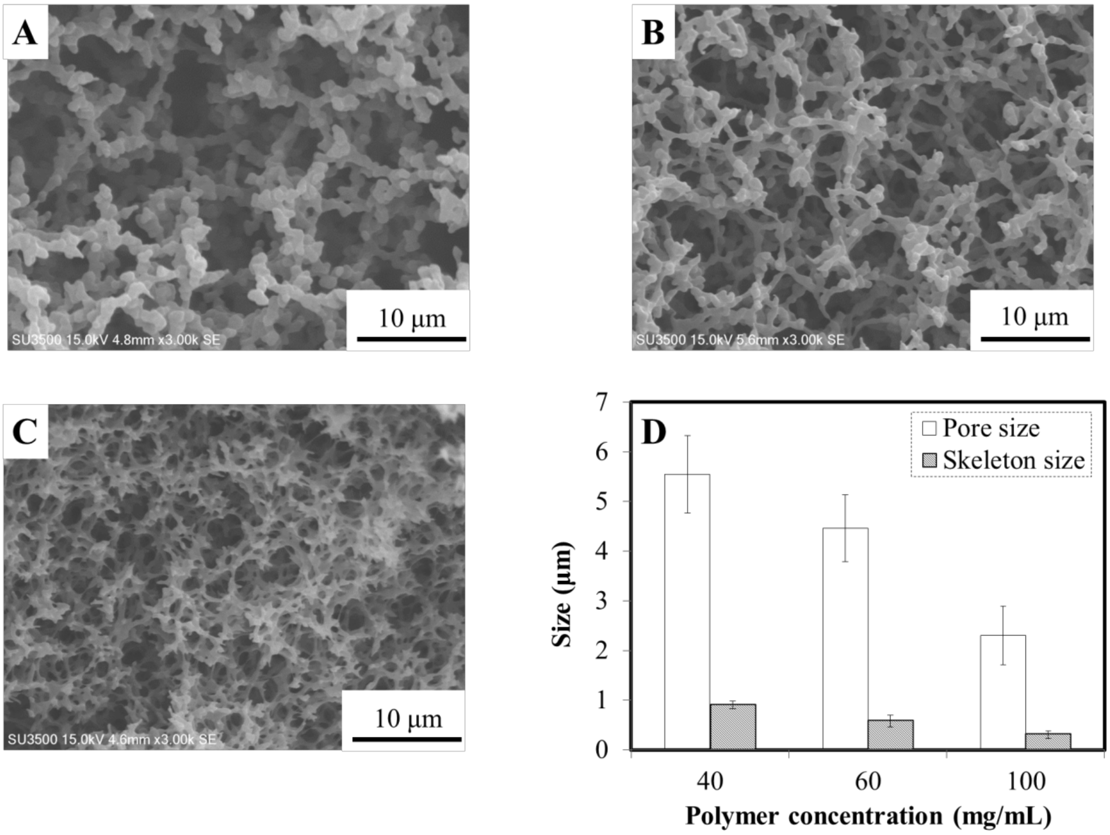

Fig. 1-7 SEM micrographs showing the effect of the polymer concentration on the morphology of PGM monolith (A) 40 mg/mL (B) 60 mg/mL (C) 100 mg/mL (D) The pore and skeleton sizes of PGM monolith at different polymer concentrations

Mechanism of forming PGM monolith

The mechanism of forming PGM monolith is explained as follows. First the polymer is dissolved due to cosolvency by heating. The polymer chains are random and extended in polymer solution at the beginning. As soon as phase separation takes place, the chains will entangle into each other and then further develop into the formation of skeleton, while the vacancy will developed into the pore structure.

The hypothesis to explain the effect of preparation conditions on the pore structure is proposed as follows. First we talk about the effect of polymer concentration. When the concentration is low, the viscosity of the solution is low. The low viscosity results in easy movement of polymer chains in the solution. Therefore, more polymer chains can get entangled to form large skeleton before the phase separation completes. In addition, the vacancy becomes large which results in large pores. Otherwise, the high concentration will result in small skeleton size.

Then we talk about the effect of cooling temperature on the pore structure. When the temperature is low, there is very short time for the polymer chain to get entangled before the phase separation terminates. That is to say, less chain can get coiled to result in small skeleton. Otherwise, the high temperature will result in large skeleton size.

1.4 Conclusion

In this chapter, PGM was synthesized by a conventional radical copolymerization. The unit ratio of MMA and GMA determined by ^{1}H NMR spectroscopy was 89/11. PGM monoliths with three-dimensional continuous interconnected porous structures were successfully fabricated through TIPS method. We found that PGM could be dissolved in the mixture of ethanol and H_2O, both of which are non-solvent of the polymer. This could be explained by the unique cosolvency effect. The morphology of PGM monolith including pore and skeleton sizes was easily tuned by varying the fabrication parameters such as cooling temperature and polymer concentration. The skeleton and pore size increased when the cooling temperature increased and polymer concentration decreased. In addition, the mechanism of the formation of PGM monolith was discussed.

References

[1]. Svec F and Frechet JM. *Science*. 1996;273(5272):205-211.

[2]. Svec F. *Journal of Chromatography A*. 2010;1217(6):902-924.

[3]. Jiang J-X, Trewin A, Su F, Wood CD, Niu H, Jones JT, Khimyak YZ, and Cooper AI. *Macromolecules*. 2009;42(7):2658-2666.

[4]. Ben T, Ren H, Ma S, Cao D, Lan J, Jing X, Wang W, Xu J, Deng F, and Simmons JM. *Angewandte Chemie*. 2009;121(50):9621-9624.

[5]. El-Kaderi HM, Hunt JR, Mendoza-Cortés JL, Côté AP, Taylor RE, O'Keeffe M, and Yaghi OM. *Science*. 2007;316(5822):268-272.

[6]. Courtois J, Byström E, and Irgum K. *Polymer*. 2006;47(8):2603-2611.

[7]. Kimmins SD and Cameron NR. *Advanced Functional Materials*. 2011;21(2):211-225.

[8]. Vlakh E and Tennikova T. *Journal of Chromatography A*. 2009;1216(13):2637-2650.

[9]. Zakaria P, Hutchinson JP, Avdalovic N, Liu Y, and Haddad PR. *Analytical Chemistry*. 2005;77(2):417-423.

[10]. Viklund C, Svec F, Fréchet JM, and Irgum K. *Chemistry of Materials*. 1996;8(3):744-750.

[11]. Mohanan JL, Arachchige IU, and Brock SL. *Science*. 2005;307(5708):397-400.

[12]. Rohr T, Hilder EF, Donovan JJ, Svec F, and Frechet JM. *Macromolecules*. 2003;36(5):1677-1684.

[13]. Potter OG, Breadmore MC, and Hilder EF. *Analyst*. 2006;131(10):1094-1096.

[14]. Bandari R, Höche T, Prager A, Dirnberger K, and Buchmeiser MR. *Chemistry-A European Journal*. 2010;16(15):4650-4658.

[15]. Nordborg A and Hilder EF. *Analytical & Bioanalytical Chemistry*. 2009;394(1):71-84.

[16]. Anderson EB and Buchmeiser MR. *ChemCatChem*. 2012;4(1):30-44.

[17]. Hasegawa G, Kanamori K, Nakanishi K, and Yamago S. *Polymer*. 2011;52(21):4644-4647.

[18]. Zhong H and El Rassi Z. *Journal of Separation Science*. 2009;32(1):10-20.

[19]. Walsh Z, Abele S, Lawless B, Heger D, Klán P, Breadmore MC, Paull B, and Macka M. *Chemical Communications*. 2008(48):6504-6506.

[20]. Bandari R, Knolle W, Prager‐Duschke A, and Buchmeiser MR. *Macromolecular Rapid Communications*. 2007;28(21):2090-2094.

[21]. Yao C, Qi L, Jia H, Xin P, Yang G, and Chen Y. *Journal of Materials Chemistry*. 2009;19(6):767-772.

[22]. Colard CA, Cave RA, Grossiord N, Covington JA, and Bon SA. *Advanced Materials*. 2009;21(28):2894-2898.

[23]. Kanamori K, Nakanishi K, and Hanada T. *Advanced Materials*. 2006;18(18):2407-2411.

[24]. Li J, Du Z, Li H, and Zhang C. *Polymer*. 2009;50(6):1526-1532.

[25]. Okada K, Nandi M, Maruyama J, Oka T, Tsujimoto T, Kondoh K, and Uyama H. *Chemical Communications*. 2011;47(26):7422-7424.

[26]. Nandi M, Okada K, and Uyama H. *Functional Materials Letters*. 2011;4(04):407-410.

[27]. Xin Y and Uyama H. *Chemistry Letters*. 2012;41(11):1509-1511.

[28]. Xin Y, Fujimoto T, and Uyama H. *Polymer*. 2012;53(14):2847-2853.

[29]. Sun X and Uyama H. *Nanoscale Research Letters*. 2013;8(1):1-5.

[30]. Sun X, Fujimoto T, and Uyama H. *Polymer Journal*. 2013;45(10):1101-1106.

[31]. Sun X and Uyama H. *Colloid & Polymer Science*. 2014;292(5):1073-1078.

[32]. Park S-B, Sakamoto J, Sung M-H, and Uyama H. *Polymer*. 2013;54(22):6114-6118.

[33]. Park S-B, Sakamoto J, Sung M-H, and Uyama H. *Polymer Degradation & Stability*. 2014;99:99-104.

[34]. González-Benito J and Koenig J. *Polymer*. 2006;47(9):3065-3072.

[35]. Everett D. *Pure & Applied Chemistry*. 1972;31(4):577-638.

[36]. Brunauer S, Deming LS, Deming WE, and Teller E. *Journal of the American Chemical Society*. 1940;62(7):1723-1732.

[37]. Brunauer S, Emmett PH, and Teller E. *Journal of the American Chemical Society*. 1938;60(2):309-319.

Chapter 2

Immobilization of horseradish peroxidase on modified PGM monolith

2.1 Introduction

Enzymes are biocatalysts having high specificity and catalytic activity under mild reaction condition and have been widely used in proteomics and chemical industry [1-3]. One of the drawbacks of enzymes is that they are easily inactivated by external factors like organic solvents, extreme temperature and pH. In addition, the use of an aqueous solution of enzymes requires the time-consuming and tedious process to separate products and enzymes. To overcome these problems, immobilization of enzymes on solid supports has been extensively studied [4-9]. So far, various materials have been used to immobilize enzymes such as membranes, beads, sol-gel supports and porous materials [10-20]. It has been shown that chemical compositions as well as morphology of the materials are the critical factors to enhance the catalytic activity, stability and reusability of enzymes.

The immobilization process plays an important role of the enzyme activity compared to that of the soluble counterpart. The physic-chemical nature of the support as well as the immobilization methods are the main factors. The support nature acts mainly *via* "partitioning effect" which is due to the changes in the chemical composition of the microenvironment where the immobilized enzyme operating compared to the soluble enzyme [21]. The immobilization method acts through the nature of the binding forces or through the type and the position of the aminoacidic residues involved in the enzyme attachment. Covalent coupling is the most convenient immobilization and reusability of the bound enzyme [22]. In addition, covalent attachment avoid relevant leaking of enzyme which takes places in repeated uses since the binding forces are stronger than those occurring in the absorption or ionic binding.

However one of the main problems associated with the use of immobilized enzymes is the loss of catalytic activity, especially due to the steric hindrance between enzyme and support. Spacer structure incorporation through enzyme and support is a common method to reduce undesirable interactions between the functional groups on the support surface and the large enzyme molecule and to lower steric hindrance [23]. Spacer structures with low-molecule weight usually consist of linear hydrocarbon chains with functionalities on both ends for the coupling to the support and enzyme [24].

Phenolic resin processing and other industrials will produce large amount of phenolic compounds which occur in the waste streams of a wide variety of industrial operations where their concentrations typically range from 100 to 1000 mg/L [25]. The majority of phenols have been regarded as toxic priority pollutants and some are known or suspected carcinogens [26]. Conventional treatment including such as solvent extraction, are high cost, low efficiency and toxic by-products [27]. Recently the use of oxidoreductive enzymes to catalyze the removal of aromatic compounds has been attractive. Especially, horseradish peroxidase (HRP) catalyzes the oxidation of aqueous phenol by hydrogen peroxide, which converts the phenol with low molecule weight and high solubility to high molecule weight and low solubility [28]. Therefore, these products precipitate from solution and can be removed by filtration in an easy way.

Polymer-based monolithic materials with interconnected porous structure have a high potential for enzyme immobilization due to their large surface area, wide pH stability and excellent biocompatibility [29]. Generally, polymer-based monoliths are prepared by polymerization of the corresponding monomers in the presence of porogens or high internal phase emulsion [30-37]. In these methods, the use of toxic additives like porogens, cross-linkers and other compounds are often required to create porous structures. Furthermore, it is difficult to obtain well-defined porous structures because both polymerization and phase separation have to be controlled simultaneously and precisely. Some other researches reported templates were utilized to prepare porous materials including biodegradable polymer or supramolecular aggregate [38-40].

In Chapter 1, a reactive PGM monolith with epoxy group was fabricated by a facile and straightforward method *via* thermally induced phase separation (TIPS) without the need of templates and additives. In TIPS method, polymers were dissolved in an appropriate solvent by heating due to cosolvency effect and thereafter cooled to induce phase separation to form a monolith.

Monolith with large surface area and interconnected pore structure is a suitable candidate support for enzyme immobilization. This chapter deals with modification of PGM monolith and immobilization of HRP. The epoxy groups of the PGM monolith is reacted with adipic acid dihydrazide (AADH) and ethylenediaminetetraacetic dianhydride (EDTAD) to yield carboxyl group-bearing PGM (PGM-COOH) monolith. The carboxyl groups of the monolith is converted to *N*-hydroxysuccineimide (NHS) ester and reacted with HRP. The enzyme activity, thermal stability and reusability of the immobilized HRP were evaluated. In addition, the effect of spacer structure on the modification of PGM monolith and immobilization of HRP will be discussed. Three different spacer structures, 1, 2-diaminoethane (2DA), 1, 6-diaminohexane (6DA) and 1, 12-diaminododecane (12DA), are selected.

2.2 Experimental

Martials

PGM was synthesized by a conventional radical copolymerization according to the protocol in Chapter 1. The molecular weight was determined to be 1.4×10^5 by size exclusion chromatography (SEC). The unit ratio of MMA and glycidyl methacrylate determined by ^{1}H NMR spectroscopy was 89/11. Adipic acid dihydrazide (AADH) was purchased from Sigma Aldrich. Ethylenediaminetetraacetic dianhydride (EDTAD), 4-aminoantipyrine (4-AAP) and 1-ethyl-3-(3-dimethylaminopropyl) carbodiimide hydrochloride (EDC) were obtained from Tokyo Chemical Industry. 1, 6-diaminohexane (6DA), 1, 12-diaminododecane (12DA), potassium ferricyanide ($FeK_3(CN)_6$), N-hydroxysuccinimide (NHS), HRP, hydrogen peroxide (H_2O_2), phenol, phosphate buffer (1/15 M, pH 7), dimethyl sulfoxide (DMSO), *N*,*N*-dimethylformamide (DMF), and ethanol were purchased from Wako Pure Chemical Industries. 1, 2-diaminoethane (2DA), acetate buffer (0.1M, pH 5) were obtained from Nacalai tesque. Coomassie (Bradford) protein assay kit was purchased from Thermo Scientific.

Instrumentation

Scanning electron microscopic (SEM) images were recorded on a Hitachi SU3500 instrument at 15kV. A thin gold film was sputtered on the samples before the images were collected. Attenuated total reflection fourier transform infrared (ATR-FT-IR) spectroscopy was performed on a Thermo Scientific Nicolet iS5 with iD5 ATR accessory. UV-vis spectroscopy was performed with a Hitachi U-2810 UV-vis spectrometer.

Preparation of PGM monolith

The PGM monolith was prepared as described in Chapter 1. A typical procedure was as follows. PGM polymer (60 mg/mL) was dissolved in a mixed solvent of ethanol/H_2O (80/20 v/v) at 60 °C. This solution was kept at 20 °C for 12 h to form the PGM monolith. This monolith was washed with deionized water three times and dried under vacuum.

Modification of PGM monolith

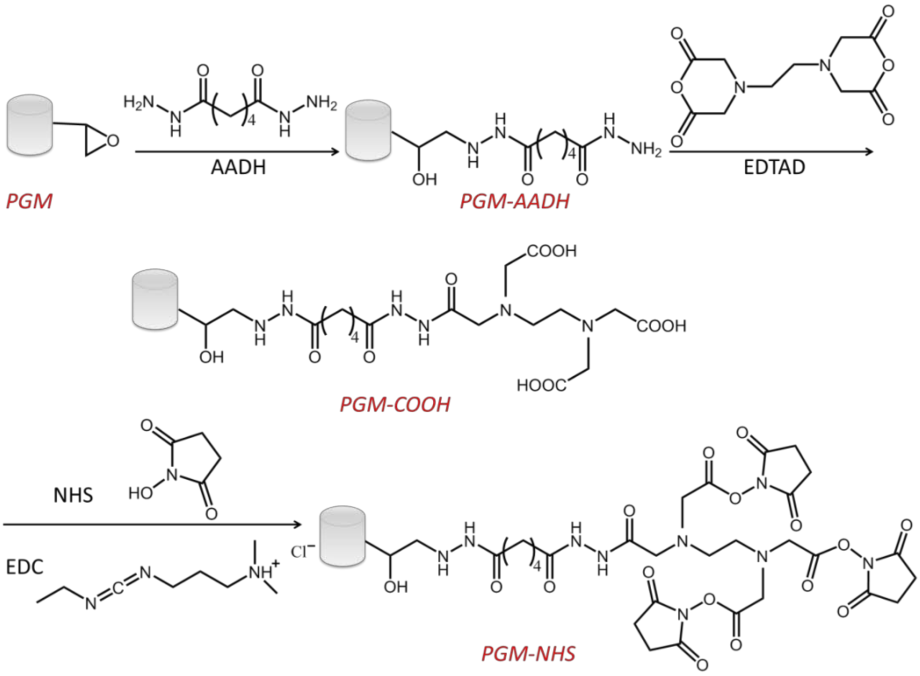

Fig. 2-1 Modification process of PGM monolith

Fig.2-1 illustrates the modification process of the PGM monolith. The PGM monolith (20 mg) was immersed in 5 mL of 0.5 M AADH solution in a mixture of acetate buffer/ethanol=1/1 (v/v) for 24 h at 60 °C. This monolith was subsequently reacted with 5 mL of 0.5 M EDTAD in anhydrous DMSO for 24 h at 60 °C to yield the PGM-COOH monolith. This monolith was reacted with 5 mL of 0.2 M EDC and 0.2 M NHS in DMF for 4 h at 40 °C. After each step of the reactions, the monolith was washed with water three times and then dried in vacuum. The amount of the NHS groups on the monolith was determined by a spectrophotometric assay at 260 nm using 0.1 M ammonium hydroxide solution (Fig. 2-2) [41].

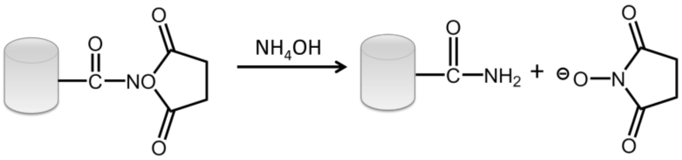

Fig. 2-2 Method for quantification of NHS ester

HRP immobilization on the PGM-NHS monolith

A typical immobilization procedure is as follows. The PGM-NHS monolith (20 mg) was immersed in 1 mL phosphate buffer (1/15 M, pH 7) containing 1 mg/mL HRP and incubated for 48 h at 15 °C under gentle shaking. The monolith was taken out and washed three times with the buffer to remove nonspecifically adsorbed HRP. The amount of HRP immobilized on the monolith was determined by measuring the concentration change of the initial and final HRP solutions using the Bradford protein assay method [42]. The absorbance at 595 nm was recorded to determine the HRP concentration.

Enzyme activity

Enzyme activity of HRP was measured using phosphate buffer (1/15 M, pH 7) containing 60 mM phenol, 14 mM 4-AAP, and 2 mM H_2O_2 [43]. As free HRP, phosphate buffer (1/15 M, pH 7) containing 5 µg/mL HRP was used. As the immobilized HRP, 20 mg of the HRP-immobilized monolith was used. The activity was determined by monitoring the absorption of a benzoquinone derivative at 510 nm. To assess the thermal stability, the immobilized and free HRP was incubated at 60 °C and the enzyme activity was measured at the different time intervals. Moreover, after measuring the enzyme activity of the immobilized HRP, the monolith was washed with phosphate buffer and the activity was measured again to evaluate the reusability of the immobilized HRP.

Modification using different diamine spacer

Even the immobilized HRP shows excellent stability and reusability, one of potential obstacles is steric interference between HRP and the support, which probably prevents HRP covalent binding [44]. As a result, spacer structure, e.g. length of spacer, could be a critical factor to reduce steric interference when HRP was immobilized on the solid support. Here three types of diamine reagents (1, 2-diaminoethane (2DA), 1, 6-diaminohexane (6DA) and 1, 12-diaminododecane (12DA)) were used to examine the effect of spacer length on the HRP immobilization (Fig. 2-3). The diamine reagent was dissolved at the concentration 10 wt% in ethanol. The PGM monolith was incubated in the diamine solution for 24 h at 60 °C to yield PGM-n-DA (n=2, 6 and 12) monolith.

This monolith was subsequently reacted with 5 mL of 0.5 M EDTAD in anhydrous DMSO for 24 h at 60 °C to yield the PGM-n-COOH monolith (n=2, 6 and 12). This monolith was reacted with 5 mL of 0.2 M EDC and 0.2 M NHS in DMF for 4 h at 40 °C. After each step of the reactions, the monolith was washed with water three times and then dried in vacuum.

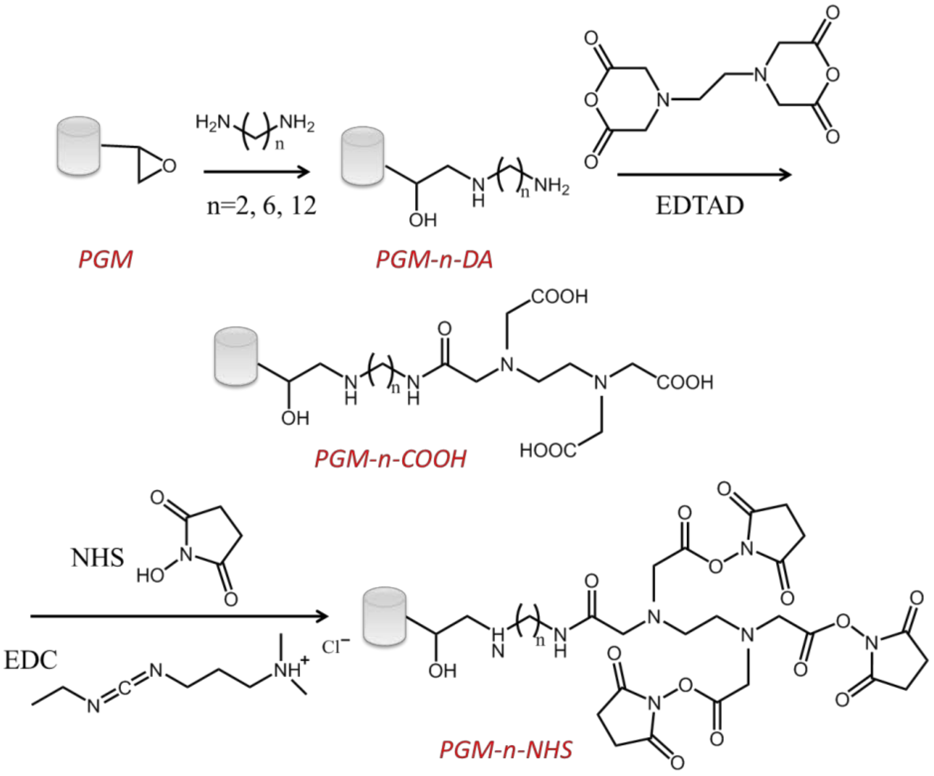

Fig. 2-3 Chemical scheme for PGM modification by spacer structure

Application for phenol removal

Phenolic compounds are toxic in the environment. One of the efficient and low cost ways to remove them is to use HRP to catalyze oxidation of phenols in aqueous media. Here, the immobilized HRP on the modified PGM monolith with the spacer was used for phenol removal. Immobilized HRP was incubated in 1 mL of a phenol substrate (containing 60 mM phenol, 20.8 mM 4-AAP and 4 mM H_2O_2) for 15 min at 15 °C. The supernatant (0.2 mL) was taken out and mixed with 1 mL of the catalase solution at the concentration of 1 mg/mL for 5 min, followed by adding into 200 μL of coagulant ($AlK(SO_4)_2$, 40 g/L). After centrifugation, 50 μL of the supernatant was taken out and mixed with 750 μL PBS, 100 μL 20.8 mM 4-AAP and 100 μL 83.4 mM ferricyanide for 5 min at 15 °C. Phenol concentrations were measured by a colorimetric method and the absorbance values were recorded at 505 nm against a blank (800 μL of PBS, 100 μL of 20.8 mM 4-AAP and 100 μL of 83.4 mM ferricyanide).

2.3 Results and Discussion

Modification of PGM monolith

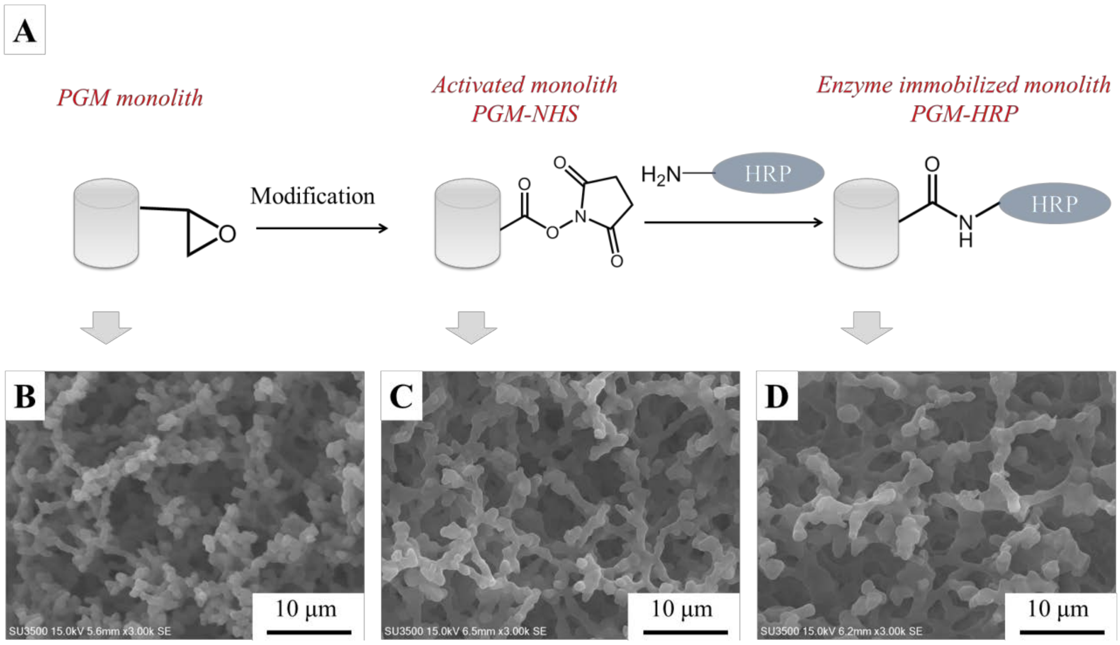

Fig.2-4 (A) Chemical scheme for preparing PGM-HRP monolith SEM images of (B) PGM monolith (C) PGM-NHS monolith (D) enzyme immobilized PGM-HRP monolith

The PGM monolith was prepared by the TIPS method. The SEM image shows the formation of the interconnected uniform pores within the PGM monolith (Fig. 2-4B). The average pore and skeleton sizes were 4.5 μm and 580 nm, respectively.

Although the epoxy group is well known to be reactive toward nucleophiles including amines, it has been reported that the immobilization of enzymes using this functional group is not efficient under mild conditions such as low ionic strength and neutral pH [45]. Therefore, we first modified the epoxy groups with AADH to yield the PGM-AADH monolith. The nitrogen content of the PGM-AADH monolith was 2%, indicating that 35% of the epoxy groups were reacted with AADH. The incomplete modification may be due to the fact that some epoxy groups were located inside the monolith backbone which was not accessible for AADH.

The PGM-AADH monolith was reacted with EDTAD and thereafter NHS. NHS was selected for efficient immobilization of an enzyme. The amount of NHS ester in the monolith was 120 nmol/mg, which indicated that 11% of hydrazine was converted into NHS group. SEM observation confirmed that the monolith had porous morphology after the modification (Fig. 2-4).

Fig. 2-5 shows the FT-IR spectra of PGM monoliths before and after the modification with AADH, EDTAD and NHS. A peak at 908 cm^{-1} was due to the epoxy group of the PGM monolith, which disappeared after the reaction with AADH (Fig. 2-5A). For the PGM-AADH monolith, a broad peak around 3544 cm^{-1} corresponding to hydrazine groups of AADH and hydroxyl group and a peak at 1660 cm^{-1} due to the amide bond were observed (Fig. 2-5B). For the PGM-COOH monolith, a peak was observed at 1592 cm^{-1} which was attributed to C=O asymmetric stretching of the carboxylate groups (Fig. 2-5C). This peak disappeared after the NHS modification (Fig.

2-5D). These data indicate the successful modification of the PGM monolith.

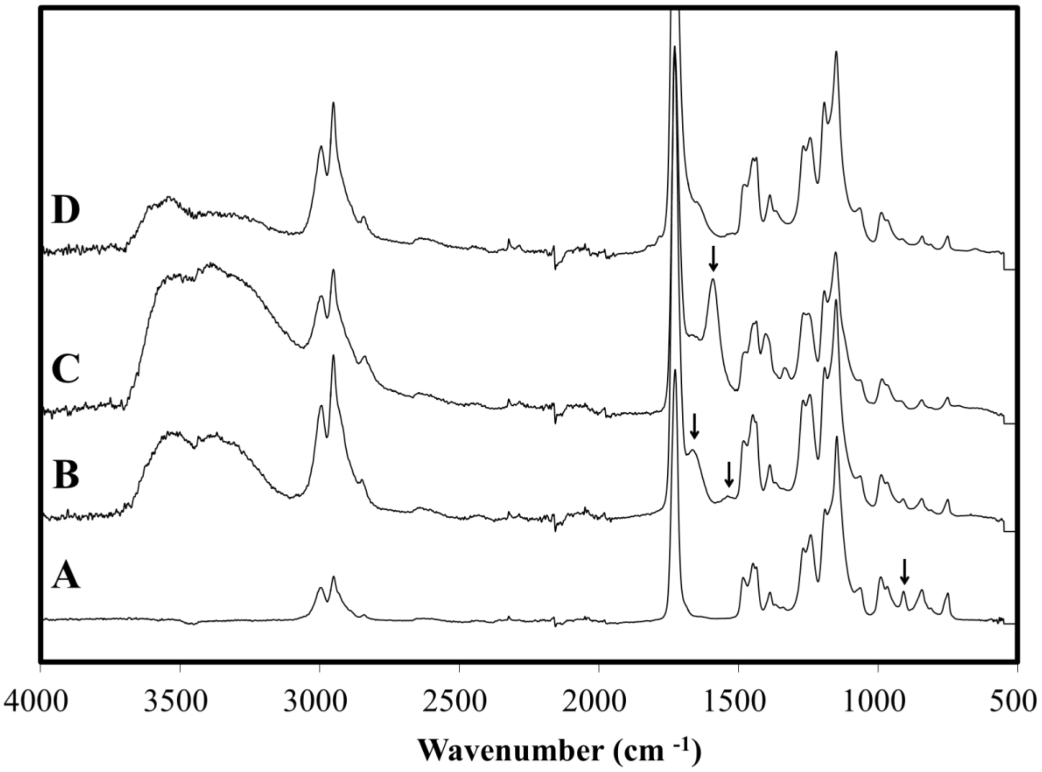

Fig.2-5 FT-IR spectra of (A) PGM monolith (B) PGM-AADH monolith (C) PGM-COOH monolith (D) PGM-NHS

HRP immobilization

There are various methods to prepare immobilized HRP on solid supports, generally speaking, physical adsorption and covalent binding. Zhang et al. reported that HRP was physically immobilized on graphene oxide (GO) by adsorption due to electrostatic interaction [46]. However, physical attachment may not be strong enough to prevent the loss of enzymes during the operation, which limits wide applications of the immobilized HRP [47]. Hence, covalent binding has attracted more and more attention. Azevedo et al. immobilized HRP on alkylamine controlled pore glass (CPG) by adsorption and covalent binding for comparison [48]. They found that HRP immobilized on CPG by adsorption was partially lost during washing procedure, while the loading amount of HRP immobilized covalently was up to 21.0 mg/g. Lai described that HRP was immobilized on porous aminopropyl glass (APG) beads by covalent binding with loading amount of 9.6 mg/g [49]. Bayramoğlu reported that HRP covalent loading amount on magnetic PGM beads was 3.4 mg/g [50]. In this study, the immobilization of HRP on the activated PGM-NHS monolith was carried out by incubating the PGM-NHS monolith in a HRP-containing buffer solution. The loading amount was up to 41.0 mg/g, which is much higher than those of many other reported solid supports.

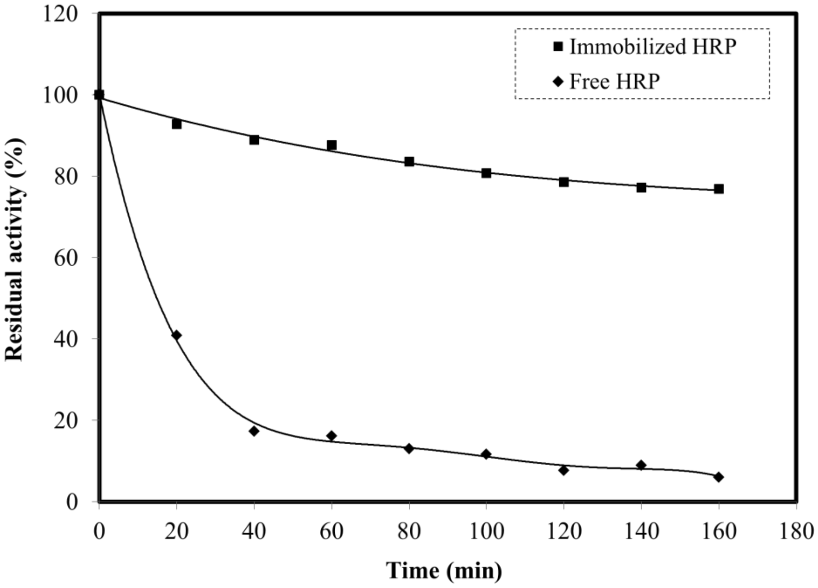

Fig.2-6 Thermal stability of the immobilized and free HRP at 60 °C

The thermal stability of the immobilized HRP was evaluated. The free and immobilized HRP was incubated at 60 °C and the enzyme activity was measured at the different time intervals. The immobilized HRP possessed much higher thermal stability than that of free HRP (Fig.2-6). The immobilized HRP kept its activity after 20 min incubation (relative activity: 93%), while the activity of free HRP decreased to 41%. Furthermore, the immobilized HRP showed 77% of the activity even after 160 min, whereas only 6% relative activity was observed for free HRP. These data clearly show that the immobilization of HRP on the monolith improves the thermal stability, probably owing to the less conformational change after the covalent immobilization.

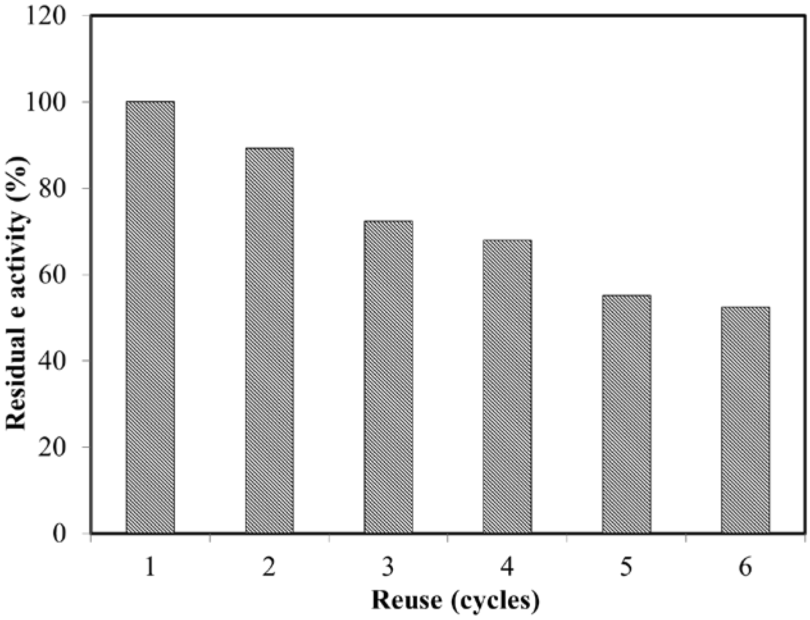

Fig. 2-7 Reusability of the immobilized HRP

One attractive advantage of immobilized enzymes is that they can be easily separated from the reaction system and reused, which greatly decreases the cost in enzymatic transformation for practical applications. After the first cycle of the catalytic reaction by the immobilized HRP, the monolith was washed and the activity was measured again. The enzyme activity of the immobilized HRP was plotted against the catalytic cycles in Fig.2-7. After 6 cycles, the enzyme activity still remained 52% of its initial activity, which is much higher than that reported by Zhang (30% on GO by adsorption) and Azevedo (7% on APG beads by covalent binding) [46, 49]. The decreased activity was probably due to the accumulation of *p*-quinoneimide, a red product of the enzymatic reactions, on the surface of the PGM monolith [51].

Effect of spacer length

The effect of spacer length on the modification of the PGM monolith and the HRP immobilization are shown in Table 2-1. The nitrogen weight percentage in PGM-2-DA (2.3%) was higher than that in 12DA (1.5%). However, the NHS ester amount in PGM-2-NHS (10 nmol/mg) was lower than that in PGM-12-NHS. Moreover, the highest HRP loading amount was found in PGM-12-NHS monolith. These results indicate that the longer spacer could reduce steric interference.

Immobilized HRP on modified monolith was used to evaluate the efficiency of phenol removal. The effect of the spacer length was shown in Table 2-1. The removal capacity of the immobilized HRP on the monolith with spacer of 12DA (1.6 mol/g) is higher than that with spacer of 2DA (1.2 mol/g). The reason could be explained as following. The larger flexibility of the longer spacer could reduce the steric interference between HRP and monolith. In addition, the attachment of the HRP to the spacer does not interfere with the amino acid residues of the catalytic site.

Table 2-1 Effect of spacer length on the modification of PGM monolith and the immobilization of HRP

	Diamine reagent			Quantification method
	2DA	6DA	12DA	
N wt% in PGM-nDA(%)	2.3	2.0	1.5	Elemental analysis
Epoxide involved in the reaction	77	67	50	
NHS ester in PGM-n-NHS(nmol/mg)	10	26	95	UV-vis
HRP loading amount (mg/g)	3	5	10	Bradford protein assay
Efficiency for phenol removal (mol/g)	1.2	1.4	1.6	UV-vis

2.4 Conclusion

In this chapter, we used the epoxide-containing polymethacrylate-based monolith having a well-defined porous structure as a solid support for the immobilization of HRP. The PGM monolith was modified with AADH, EDTAD and NHS to introduce the reactive NHS ester groups, followed by reacting with HRP under mild reaction conditions. The immobilized HRP on the modified PGM monolith showed enhanced thermal stability at 60^{o}C and kept 52% of the original activity after 6 cycles of the reaction.

Furthermore, three spacers with different lengths were selected to modified PGM monolith. Moreover, the spacer structure could reduce the steric interference when HRP was immobilized on modified PGM monolith.

References

[1]. Pollard DJ and Woodley JM. *Trends in Biotechnology*. 2007;25(2):66-73.

[2]. Woodley JM. *Trends in Biotechnology*. 2008;26(6):321-327.

[3]. Schmid A, Dordick J, Hauer B, Kiener A, Wubbolts M, and Witholt B. *Nature*. 2001;409(6817):258-268.

[4]. Sheldon RA. *Advanced Synthesis & Catalysis*. 2007;349(8 ‐ 9):1289-1307.

[5]. Bornscheuer UT. *Angewandte Chemie International Edition*. 2003;42(29):3336-3337.

[6]. Cao L. *Current Opinion in Chemical Biology*. 2005;9(2):217-226.

[7]. Garcia ‐ Galan C, Berenguer ‐ Murcia Á, Fernandez ‐ Lafuente R, and Rodrigues RC. *Advanced Synthesis & Catalysis*. 2011;353(16):2885-2904.

[8]. Luckarift HR, Spain JC, Naik RR, and Stone MO. *Nature Biotechnology*. 2004;22(2):211-213.

[9]. Lei C, Shin Y, Liu J, and Ackerman EJ. *Journal of the American Chemical Society*. 2002;124(38):11242-11243.

[10]. Chen B, Pernodet N, Rafailovich MH, Bakhtina A, and Gross RA. *Langmuir*. 2008;24(23):13457-13464.

[11]. Klein MP, Nunes MR, Rodrigues RC, Benvenutti EV, Costa TM, Hertz PF, and Ninow JL. *Biomacromolecules*. 2012;13(8):2456-2464.

[12]. Zhang J, Zhang F, Yang H, Huang X, Liu H, Zhang J, and Guo S. *Langmuir*. 2010;26(9):6083-6085.

[13]. Letant SE, Hart BR, Kane SR, Hadi MZ, Shields SJ, and Reynolds JG. *Advanced Materials*. 2004;16(8):689-693.

[14]. DeLouise LA and Miller BL. *Analytical Chemistry*. 2005;77(7):1950-1956.

[15]. 15Wu L, Yuan X, and Sheng J. *Journal of Membrane Science*. 2005;250(1):167-173.

[16]. Juang R-S, Wu F-C, and Tseng R-L. *Bioresource Technology*. 2001;80(3):187-193.

[17]. Taqieddin E and Amiji M. *Biomaterials*. 2004;25(10):1937-1945.

[18]. Zou Y, Xiang C, Sun L-X, and Xu F. *Biosensors & Bioelectronics*. 2008;23(7):1010-1016.

[19]. Pierre SJ, Thies JC, Dureault A, Cameron NR, van Hest JC, Carette N, Michon T, and Weberskirch R. *Advanced Materials*. 2006;18(14):1822-1826.

[20]. Monzo A, Sperling E, and Guttman A. *TrAC Trends in Analytical Chemistry*. 2009;28(7):854-864.

[21]. Atkinson T, Scawen MD, and P.M.Hammond. in H.J.Rehm, G.Reed(Eds.), Biotechnologh. Weinheim. *VCH*, 1987.

[22]. H.H.Weetall. R.A.Messing (Ed.), Immobilized enzyme for industrial reaction New York. *Academic Press*, 1995.

[23]. Bulmuş V, Ayhan H, and Pişkin E. *Chemical Engineering Journal*. 1997;65(1):71-76.

[24]. Hermanson G, Mallia A, and Smith P. Immobilized affinity ligand techniques. 1992. Academic Press New York. G Kim, BA Kairdolf, J Li, C Chen, L Chu and SM Nie,―Targeted Cancer Nanotherapeutics,‖ Emory-Georgia Tech Frontiers of Cancer Nanotechnology Symposium: March, vol. 27, 2006. pp. 2002-2003.

[25]. Faust SD and Aly OM. Chemistry of water treatment. *CRC Press*, 1998.

[26]. Verschueren K. Handbook of environmental data on organic chemicals: Vol. 1.

John Wiley and Sons, Inc, 2001.

[27]. Rengaraj S, Moon S-H, Sivabalan R, Arabindoo B, and Murugesan V. *Journal of Hazardous Materials*. 2002;89(2):185-196.

[28]. Buchanan ID, Nicell JA, and Wagner M. *Journal of Environmental Engineering*. 1998;124(9):794-802.

[29]. Nordborg A and Hilder EF. *Analytical & Bioanalytical Chemistry*. 2009;394(1):71-84.

[30]. Hasegawa G, Kanamori K, Nakanishi K, and Yamago S. *Polymer*. 2011;52(21):4644-4647.

[31]. Svec F. *Journal of Chromatography A*. 2010;1217(6):902-924.

[32]. Walsh Z, Abele S, Lawless B, Heger D, Klán P, Breadmore MC, Paull B, and Macka M. *Chemical Communications*. 2008(48):6504-6506.

[33]. Bandari R, Knolle W, and Buchmeiser MR. *Journal of Chromatography A*. 2008;1191(1):268-273.

[34]. Li J, Du Z, Li H, and Zhang C. *Polymer*. 2009;50(6):1526-1532.

[35]. Colard CA, Cave RA, Grossiord N, Covington JA, and Bon SA. *Advanced Materials*. 2009;21(28):2894-2898.

[36]. Kanamori K, Nakanishi K, and Hanada T. *Advanced Materials*. 2006;18(18):2407-2411.

[37]. Wan Y, Wu H, Cao X, and Dalai S. *Polymer Degradation & Stability*. 2008;93(10):1736-1741.

[38]. Dai C-F, Weng C-J, Li P-R, and Yeh J-M. *Polymer Degradation & Stability*. 2010;95(4):600-609.

[39]. Shum AW, Li J, and Mak AF. *Polymer Degradation & Stability*.

2005;87(3):487-493.

[40]. Wan Y, Shi Y, and Zhao D. *Chemistry of Materials*. 2007;20(3):932-945.

[41]. Miron T and Wilchek M. *Analytical Biochemistry*. 1982;126(2):433-435.

[42]. Bradford MM. *Analytical Biochemistry*. 1976;72(1):248-254.

[43]. Patel AC, Li S, Yuan J-M, and Wei Y. *Nano Letters*. 2006;6(5):1042-1046.

[44]. Cao T, Wang A, Liang X, Tang H, Auner GW, Salley SO, and Ng K. *Biotechnology & Bioengineering*. 2007;98(6):1109-1122.

[45]. Mateo C, Fernández-Lorente G, Abian O, Fernández-Lafuente R, and Guisán JM. *Biomacromolecules*. 2000;1(4):739-745.

[46]. Zhang F, Zheng B, Zhang J, Huang X, Liu H, Guo S, and Zhang J. *The Journal of Physical Chemistry C*. 2010;114(18):8469-8473.

[47]. Lv Y, Lin Z, Tan T, and Svec F. *Biotechnology & Bioengineering*. 2014;111(1):50-58.

[48]. Azevedo A, Vojinović V, Cabral J, Gibson T, and Fonseca L. *Journal of Molecular Catalysis B: Enzymatic*. 2004;28(2):121-128.

[49]. Lai Y-C and Lin S-C. *Process Biochemistry*. 2005;40(3):1167-1174.

[50]. Bayramoğlu G and Arıca MY. *Journal of Hazardous Materials*. 2008;156(1):148-155.

[51]. Nakamoto S and Machida N. *Water Research*. 1992;26(1):49-54.

Chapter 3

Pepsin immobilization on an aldehyde-modified polymethacrylate monolith and its application for protein analysis

3.1 Introduction

Proteomics in general deals with the large-scale determination of gene and cellular function directly at the protein level [1]. Therefore, proteomics can be applied to protein profiling, protein interactions and analysis of protein modifications [2-6]. Proteomics significantly contributed to the understanding of biological processes that are essential for life, such as disease biomarker discovery, biopharmaceutical product development and system biology [7, 8].

Several proteomics approaches are available that are defined by the level (protein or peptide) at which analysis takes place (shown in Fig. 3-1) [9]. Improvement of mass spectrometry (MS) instrumentation now allow for the direct analysis of proteins. In such a so-called top-down experiment, purified proteins are detected intact and following fragmentation using different dissociation, providing information on intact protein mass and amino acid sequence [10, 11]. Top-down analysis of intact proteins reduces sample preparation to a minimum and preserves information that is sometimes lost in other proteomics strategies, such as the connectivity of multiple post-translational modifications, but is relatively insensitive [12]. Despite the clear advantages of top-down proteomics, the development of MS instrumentation is a limitation.

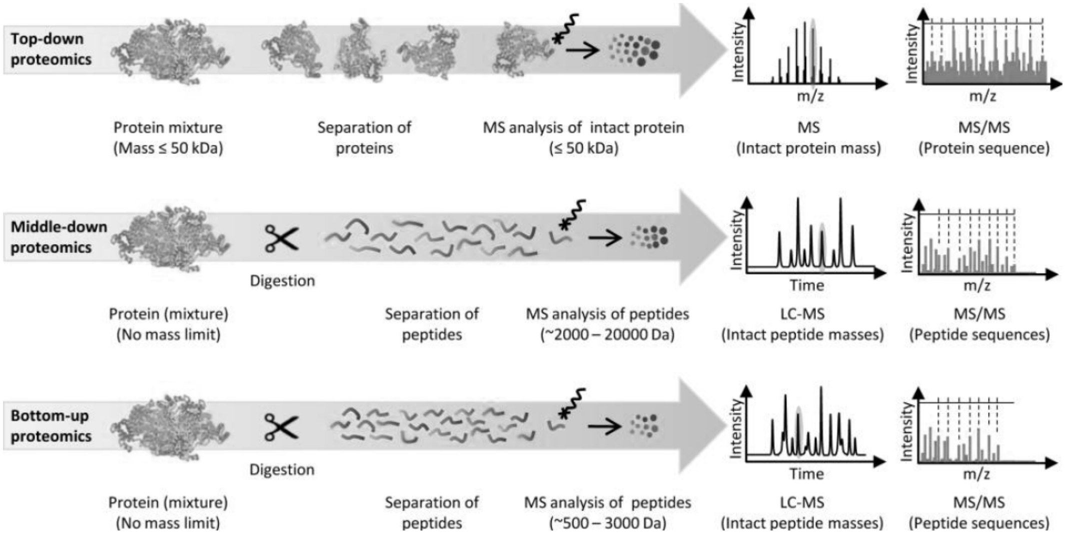

Fig. 3-1 Overview of the proteomics approaches [9]

The most of proteomics experiments rely on digestion of the protein into peptides prior to MS analysis. Compared to proteins, the analysis of peptides has several advantages including more efficient separation by liquid chromatography (LC), a lower molecular mass and fewer charge states, resulting in improvements in sensitivity [13]. Depending on the size of the produced peptides, the method is regarded as either bottom-up proteomics or middle-down proteomics. In a bottom-up approach, the protein is digested to peptides, followed by analyzed with liquid chromatography-electrospray ionization MS (LC/ESI-MS). Protein identification is performed based on peptide mass fingerprinting or peptide sequence analysis[14].

Protein digestion is a crucial step in both bottom-up and middle-down proteomics strategies and has a significant influence on the quality of protein identification [15]. Nowadays protein digestion has been improved through the development of novel techniques to increase throughput and reproducibility.

The classical approaches for protein digestion are enzymatic digestion involving proteolytic enzymes, nonenzymetic digestion utilizing chemicals and are mostly performed in-solution or in-gel. However, the most widely applied method for protein digestion involves the use of enzymes. Many enzymes which have their own characteristics in terms of specificity, efficiency and optimum digestion are available for this purpose.

The conventional protein digestions, in general, are performed in a solution which has several drawbacks such as time-consuming procedures to separate digested products from substrates and high-cost due to the difficulty in reuse of the enzyme. To solve these limitations, several techniques have been developed for rapid and efficient protein digestion, such as microwave-assisted protein digestion and using immobilized enzyme [16-19].

Enzyme immobilization is an effective approach to solve the problems as mentioned above. Four major advantages of the immobilized enzyme are as follows: improved enzyme stability; (2) increased volume specific enzyme loading; (3) simple enzyme recycling procedures and (4) facile downstream processing [20]. Taking the downstream processing as an example, immobilized enzymes could be used for protein digestion followed by liquid chromatography tandem system coupled with mass spectrometry (LC-MS) to perform efficient high-throughput analysis [21-23]. Moreover, efficient protein digestion has been reported for immobilized enzymes on various supports, such as porous matrix, sol-gel supports, nanofibers, beads and membranes [24-28].

Recently, polymer-based porous monolithic materials with large surface area have attracted more attention as solid supports for enzyme immobilization [29, 30]. Up to now, polymer-based monoliths are generally prepared from corresponding monomers by polymerization within high internal phase emulsion templates and polymerization-induced phase separation [31-39]. These methods generally require complicated and time-consuming procedures. In addition, toxic additives like cross-linkers, porogens and other template materials are used to induce porous structure. Furthermore, it is often difficult to prepare well-defined pore structure because simultaneous and accurate control of both polymerization processes and phase separation is not straightforward.

Polymethacrylate monoliths were successfully fabricated *via* the TIPS method in Chapter 1. The porous structure of PGM monolith was controlled by changing polymer concentration and cooling temperature. In Chapter 2, it was demonstrated that the high enzyme loading capacity of PGM as support for enzyme immobilization. In this chapter, we aimed to use an epoxide-containing PGM monolith, as a solid support for enzyme immobilization and apply it for online digestion system.

In this chapter, pepsin is selected as a model protein, because it is not only a well-characterized enzyme, but also one of the most important digestive enzymes. Pepsin is an aspartic endopeptidase characterized by two aspartic acid moieties within its catalytic center. It catalyzes the cleavage of peptide bonds limitation *via* hydrolysis and exhibits its maximum activity under acidic conditions [40].

Smaller fragments of the immunoglobulin (IgG) are generated enzymatically to simplify the analytical task. The analysis of IgG fragments reduces the complexity of the sample and provides more detailed information on the identification of IgG. Generally speaking, there are two strategies for the formation of fragments of the intact IgG: 1) cleavage in the hinge region using enzyme mainly pepsin and 2) disruption of disulfide bonds between light and heavy chains. After that, the peptides are directly injected into UPLC to conduct the separation procedure and followed by ESI-MS, which is online analysis to provide detailed structural information. ESI-MS spectra of IgG show multiply charged ions, and data are often represented after deconvolution, for which parameters have to be set properly to avoid signal artifacts [41].

To further explore the potential for analysis of protein primary and higher-order structures, immunoglobulin (IgG) was digested by the immobilized pepsin and analyzed by LC-MS and LC-MS/MS.

3.2 Experimental

Materials

PGM was synthesized by a conventional radical copolymerization of glycidyl methacrylate and methyl methacrylate as reported previously (41). Pepsin, hemoglobin, sodium cyanoborohydride ($NaBH_3CN$), and ethanolamine were purchased from Sigma-Aldrich (Missouri, USA). Hydrochloric acid (HCl), trichloroacetic acid (TCA), sodium chloride (NaCl), and citrate acid were purchased from Nacalai tesque (Kyoto, Japan). Tris(2-carboxyethyl)phosphine (TCEP), guanidine hydrochloride (guanidine HCl) and water were purchased from Wako Pure Chemical Industries (Osaka, Japan). Adalimumab (human IgG1) was purchased from Eisai Co. (Kyoto, Japan). Acetonitrile (ACN) and 98-100% formic acid (FA) Suprapur® were purchased from Merck Millipore International (Darmstadt, Germany).

Instrumentation

Scanning electron microscopic (SEM) images were recorded on a Hitachi SU3500 instrument (Tokyo, Japan) at an accelerating voltage of 15 kV. A thin gold film was sputtered on the samples before the images were collected. The Fourier transform infrared (FT-IR) spectra were recorded on a Thermo Scientific iD5 diamond attenuated total reflectance (ATR) for Nicolet iS5 FT-IR spectrometer (Illinois, USA). Hemoglobin solution was centrifuged using Beckman Coulter Allegra X-15R Benchtop Centrifuge (California, USA). The PGM-CHO monolith was ground by TOMY Micro Smash MS-100 (Tokyo, Japan). The ground PGM-CHO monolith was packed into a column with 0.1% FA at flow rate of 1.0 mL/min on an Alliance$^{®}$ high performance liquid chromatography (HPLC) system (Waters, Massachusetts, USA). The HPLC column (50 × 2.1 mm, w/2 μm, frit) was purchased from Grace Davison Discovery Sciences (Illinois, USA). UV spectrometry was done at 22 °C with a single beam Beckman DU-530 UV spectrophotometer (California, USA). Acquity ultra performance liquid chromatography (UPLC) equipped with a 1.0 mm × 100 mm, 1.7 mm BEH C18 column was used (Waters, Massachusetts, USA). The UPLC system was coupled to a Synapt G1 high definition mass spectrometer, equipped with an electrospray ionization source (ESI) (Waters, Massachusetts, USA).

Preparation of aldehyde-bearing PGM (PGM-CHO) monolith

The PGM monolith was prepared *via* TIPS method as described in Chapter 1. A typical procedure is as follows: 90 mg PGM powder was dissolved in 1.5 mL mixture of ethanol/water (80/20 v/v) at 60 °C, and the homogenous solution was cooled down to 20 °C to induce phase separation. The PGM monolith was obtained as a white solid. This monolith was washed with deionized water to remove ethanol and dried in vacuum.

Introduction of an aldehyde group on the PGM monolith was performed according to Fig. 3-1. The monolith (0.3 g) was immersed in dry methanol (15.0 g) containing 3.0 g of aminoacetal at 35 °C for 20 h, followed by the acidic hydrolysis of acetal groups in 10 mM HCl solution (20 mL) at 20 °C for 20 h. The resulting PGM-CHO monolith was washed with deionized water three times and dried in vacuum.

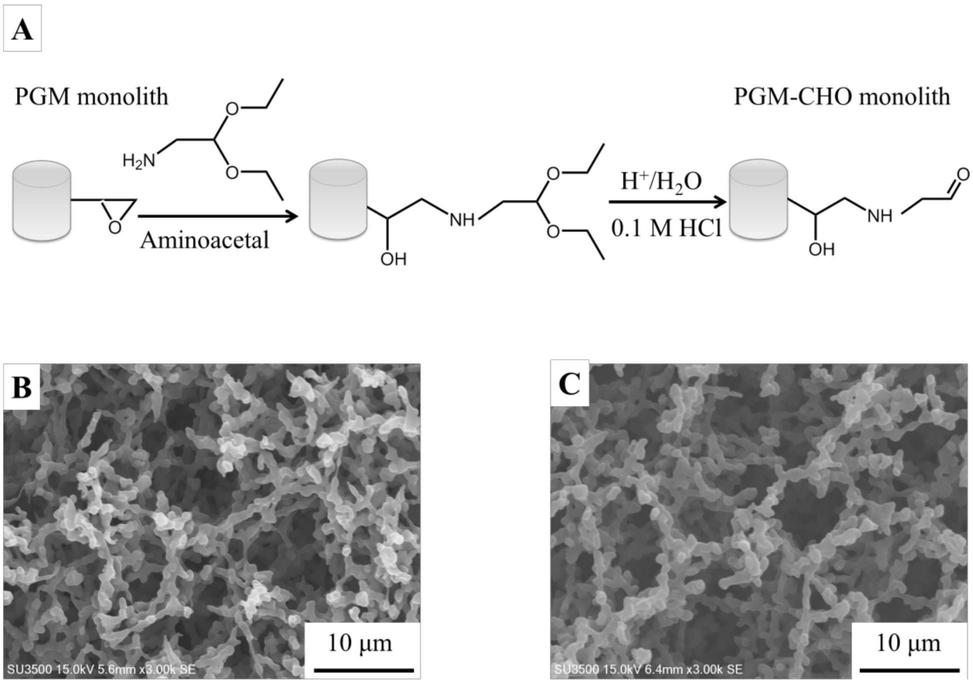

Fig. 3-1 (A) Chemical scheme for preparing the PGM-CHO monolith. SEM images of PGM monolith (B) and PGM-CHO monolith (C)

Pepsin immobilization

The pepsin was immobilized onto the PGM-CHO monolith according to the literature procedure [42]. Briefly, 200 μL of a pepsin solution (70 mg/mL) and 33 μL of 0.1 M $NaCNBH_3$ were mixed gently in an Eppendorf tube, followed by slowly adding 115 μL of 1.5 M Na_2SO_4. Then 30.0 mg monolith was added to the solution. Finally, 230 μL of 1.5 M Na_2SO_4 was added into the tube dropwise. The tube was kept for 16 h at 4 °C. To modify the unreacted aldehyde groups, 50 μL of 0.1 M ethanolamine in citrate buffer (50 mM, pH 4.4) was added into the tube and then incubated for 6 h at 4 °C. The pepsin concentration was calculated based on the absorbance at 278 nm.

Evaluation of activity of free and immobilized pepsin

The proteolytic activity of free and immobilized pepsin was determined by quantifying the amount of acid-soluble tyrosine and tryptophan residues released from denatured hemoglobin [43]. The denatured hemoglobin was prepared briefly as follows: hemoglobin was dissolved at 5 mg/mL in H_2O and centrifuged at 1000 g for 10 min. The supernatant was mixed with 0.3 M HCl at the volume ratio of 4:1.

The pepsin solution was prepared at the concentration of 92 mg/mL in citrate buffer (pH 4.4). 5 μL pepsin solution was mixed with 133 μL buffer and kept for 10 min. The influence of the temperature was studied by incubating the mixture at different temperature (30-80 °C) at pH 3 in 10 mM HCl, while the effect of pH was investigated using citrate buffer solution of different pH (pH 2-7) at 40 °C. Afterwards, 267 μL hemoglobin substrate solution was added. The reaction was incubated at 40 °C for 3 min and then quenched by the adding of 5% (w/v) TCA/H_2O solution. After centrifuging, the pepsin activities were estimated from the increase of UV absorbance at 280 nm in supernatant.

The immobilized pepsin on the PGM-CHO monolith (30.0 mg) was incubated in 200 μL buffer for 10 min. The influence of the temperature was studied by incubating the mixture at different temperature (30-80 °C) at pH 3 in 10 mM HCl, while the effect of pH was investigated using citrate buffer solution of different pH (pH 2-7) at 40 °C. Afterwards, 400 μL hemoglobin substrate solution was added. The reaction was incubated at 40 °C for 3 min and then quenched by the adding of 5% (w/v) TCA/H_2O solution. After centrifuging, the pepsin activities were estimated from the increase of UV absorbance at 280 nm in supernatant. The data were normalized by setting the highest data point in each curve as 100%.

Online analysis using pepsin monolith column via UPLC-ESI-MS/MS

PGM-CHO monolith was ground at 2400 rpm for 1 min, followed by selecting using sieve with size of 57 μm. The ground PGM-CHO monolith (30 mg) was immobilized with pepsin following the protocols as mentioned above. Afterwards, the monolith with immobilized pepsin, which was suspended in 100 μL citrate buffer (pH 4.4), was added into HPLC column. The pepsin monolith column was equipped into HPLC with 0.1% FA as an eluent at a flow rate of 1 mL/min for 30 min.

The online digestion platform is shown in Fig. 3-2. IgG was dissolved at a concentration of 2 μM. Then, the denaturing/reduction buffer (100 mM sodium phosphate, 150 mM NaCl, 4 M guanidine HCl, and 500 mM TCEP) was added twice of the IgG solution volume. The denatured and reduced samples were injected into a Waters HDX system followed by digestion by flowing through an online immobilized pepsin column. The resulting peptide mixture was desalted on a Waters VanGuard precolumn at a flow rate of 100 μL/min for 5 min and then separated in a reverse phase UPLC column at a flow rate of 40 μL/min. ACN gradient with 0.1% FA from 8% to 40% was used to peptide separation. The eluent was directly injected into a Synapt G1 mass spectrometer running in the ESI positive mode. The data were acquired in full MS scan over a range of 100 < m/z < 2000 with lock mass spray correction using Glu-fibrinogen B peptide. The peptides resulting from online pepsin digestion were also measured by running a separate experiment to collect tandem (MS/MS) mass spectrometry data. The MS/MS data were analyzed using the Waters ProteinLynx Global Server (PLGS) to identify peptides. Commercial pepsin column (POROS column, Poroszyme® Immobilized Pepsin Cartridge, 2.1 mm × 30 mm) was used in this experiment as a control.

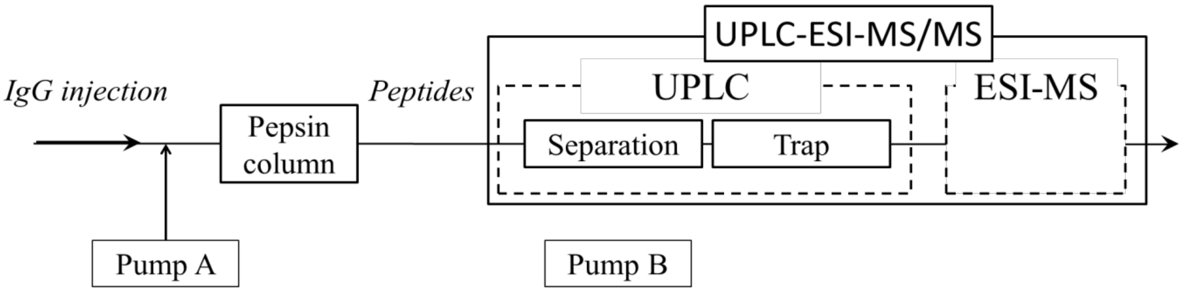

Fig. 3-2 Online digestion platform. IgG is loaded with pump A (0.05% FA in H_2O) and digested through pepsin column. ACN gradient with 0.1% FA from 8% to 40% (pump B) was used to peptide separation. The eluent was directly injected into a Synapt G1 mass spectrometer running in the ESI positive mode.

3.3 Results and Discussion

Pepsin immobilization on PGM monolith

It has been reported that even though an epoxy group is known to react with amines, the reactivity is low under a mild condition which is not feasible for enzyme immobilization [44]. Therefore, we modified the epoxide group in the PGM monolith with aminoacetal followed by acid hydrolysis of the acetal group to yield an aldehyde-bearing PGM (PGM-CHO) monolith (Fig. 3-1A).

Table 3-1 Elemental analysis result of PGM-CHO monolith

	Element (weight percentage %)		
	H	C	N
The PGM monolith	7.57	59.28	0
The PGM-CHO monolith	7.56	56.37	0.76

Fig. 3-3 shows the FT-IR spectra of the PGM monolith before and after the modification. The peak at 908 cm^{-1} due to the epoxy group disappeared after the reaction. The new peaks assignable to an amino group were observed around 1630 cm^{-1} (N-H bend) and 3500 cm^{-1} (N-H stretch). The elemental analysis (in Table 3-1) indicated that the 50% of the epoxy group was converted to the aldehyde group. Furthermore, SEM image shows little significant change in the structure of the monolith before and after the modification (Fig. 3-1B and C). The C=O stretching corresponding to aldehydes on PGM-CHO, which are typically observed in the range of 1735 cm^{-1}, was overlapped because of the strong and sharp peak assigned to C=O in PGM.

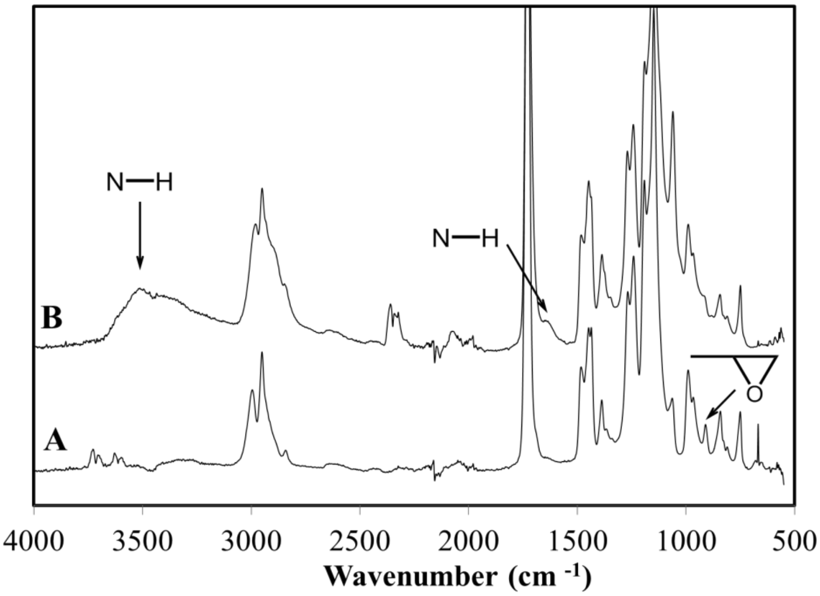

Fig. 3-3 FT-IR spectra of PGM monolith (A) and PGM-CHO monolith (B)

Next, the pepsin was immobilized onto the PGM-CHO monolith by reductive amination of the aldehyde group of the PGM-CHO monolith and the amino group of pepsin. The amount of pepsin immobilized onto the monolith was 137 mg/g, which is higher than that reported in the literature [45].

Influence of temperature and pH on activity of free and immobilized pepsin

The activity of free and immobilized pepsin was compared at different temperatures (Fig. 3-4). The optimum temperature for the immobilized pepsin was 60 °C, which was much higher than that for the free pepsin. The relative activity was above 50% at the temperature in the range of 30-70 °C for the immobilized pepsin. On the other hand, the increase of temperature significantly reduced the activity of free pepsin. At 70 °C, enzymatic activity was not observed for free pepsin. These results suggest the improvement of the thermal stability of pepsin by the immobilization on the monolith.

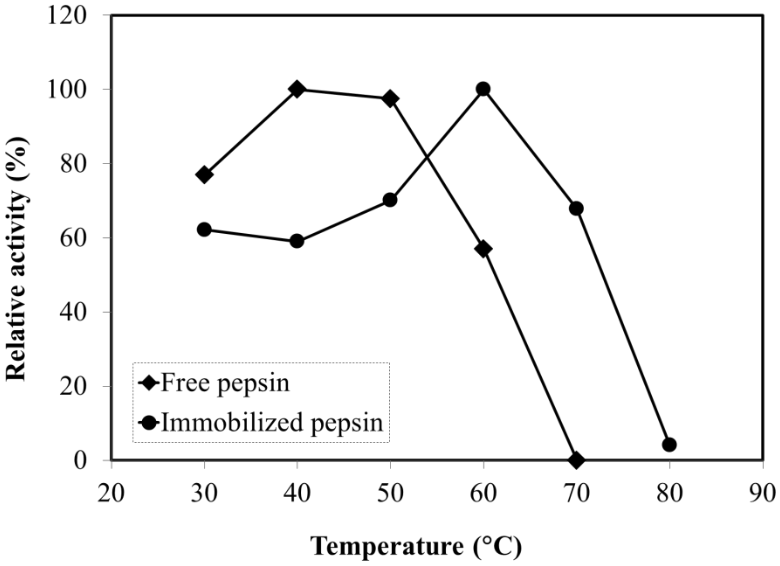

Fig. 3-4 Activity of free and immobilized pepsin at different temperatures

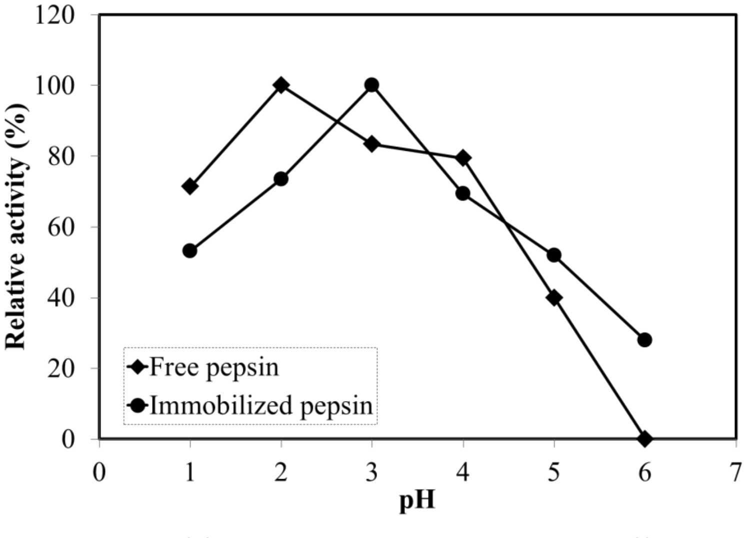

Fig. 3-5 Activity of free and immobilized pepsin at different pH

The activity of free and immobilized pepsin was compared at different pH (Fig. 3-5). The optimum pH for the immobilized pepsin was pH 3, whereas the highest activity was observed at pH 2 for free pepsin. Furthermore, the relative activity of the immobilized pepsin was above 50% in the wide pH range (pH 1-5) while the activity of free pepsin showed significant decrease at pH above 5. This difference may be owing to the conformational change of pepsin immobilized on the monolith.

These results suggest that the monolith can inhibit irreversible denaturation and aggregation of pepsin at high temperature as well as neutral pH. The improved stability against pH and temperature may be due to the space confinement in the solid support, which prevents protein denaturation and/or aggregation [46]. Thus, the present study will expand usage of monoliths as enzyme supports in various bio-related applications.

Online digestion through pepsin monolith column for UPLC-ESI-MS/MS

As the improved stability of immobilized pepsin was demonstrated, the monolith with the immobilized pepsin is packed into a column and explored its potential in the UPLC-ESI-MS/MS online digestion system. PGM-CHO monolith was ground at 2400 rpm for 1 min, followed by collecting the piece using sieve with size of 57 μm. The pepsin was immobilized on the ground PGM-CHO monolith following the protocols as mentioned above. Afterwards, the monolith with immobilized pepsin, which was suspended in 100 μL citrate buffer (pH 4.4), was added into a HPLC column. The pepsin monolith column was equipped into HPLC with 0.1% FA as an eluent at a flow rate of 1 mL/min for 30 min.

The backpressure of the PGM monolith column at around 200 psi was much lower than that of the POROS column at around 260 psi when the LC-MS experiment was conducted, which is probably because that the monolith column has better mass transfer than the POROS column. Moreover, the backpressure of the monolith was very stable during the experiment probably due to the good mechanical strength of the monolith column.

Base peak ion chromatography at set mass range of 100–2000 m/z for IgG peptic fragments produced by the digestion through the online pepsin immobilized monolith column were shown in Fig. 3-6. Here MS spectra were obtained in positive ESI mode. The peptides with low molecular mass could be well separated in less than 3 minutes. Three repetitive measurements showed almost same chromatographic patterns, indicating the high reproducibility of the pepsin monolith column. As shown in Fig. 3-7, the pepsin monolith column provided peptides with a variety of different amino acid lengths, which is highly effective for the protein higher-order characterization including hydrogen/deuterium exchange mass spectrometry because detailed information on the target protein can be derived from peptic peptides with different lengths [47]. In addition, the number of peptides identified from the MS/MS experiments was greater in case of the pepsin monolith column, compared to a commercially available pepsin-immobilized column (POROS column) (Fig. 3-6 and 3-7). The percent coverage was then calculated by dividing the number of amino acid contained in the identified peptides in the MS/MS experiment by the total number of amino acids in the IgG. The peptides generated using the pepsin monolith column covered 99.8% of the total amino acid length of the IgG, which is equivalent coverage rate to the case when the peptides were generated by the pepsin POROS column (Table 3-2).

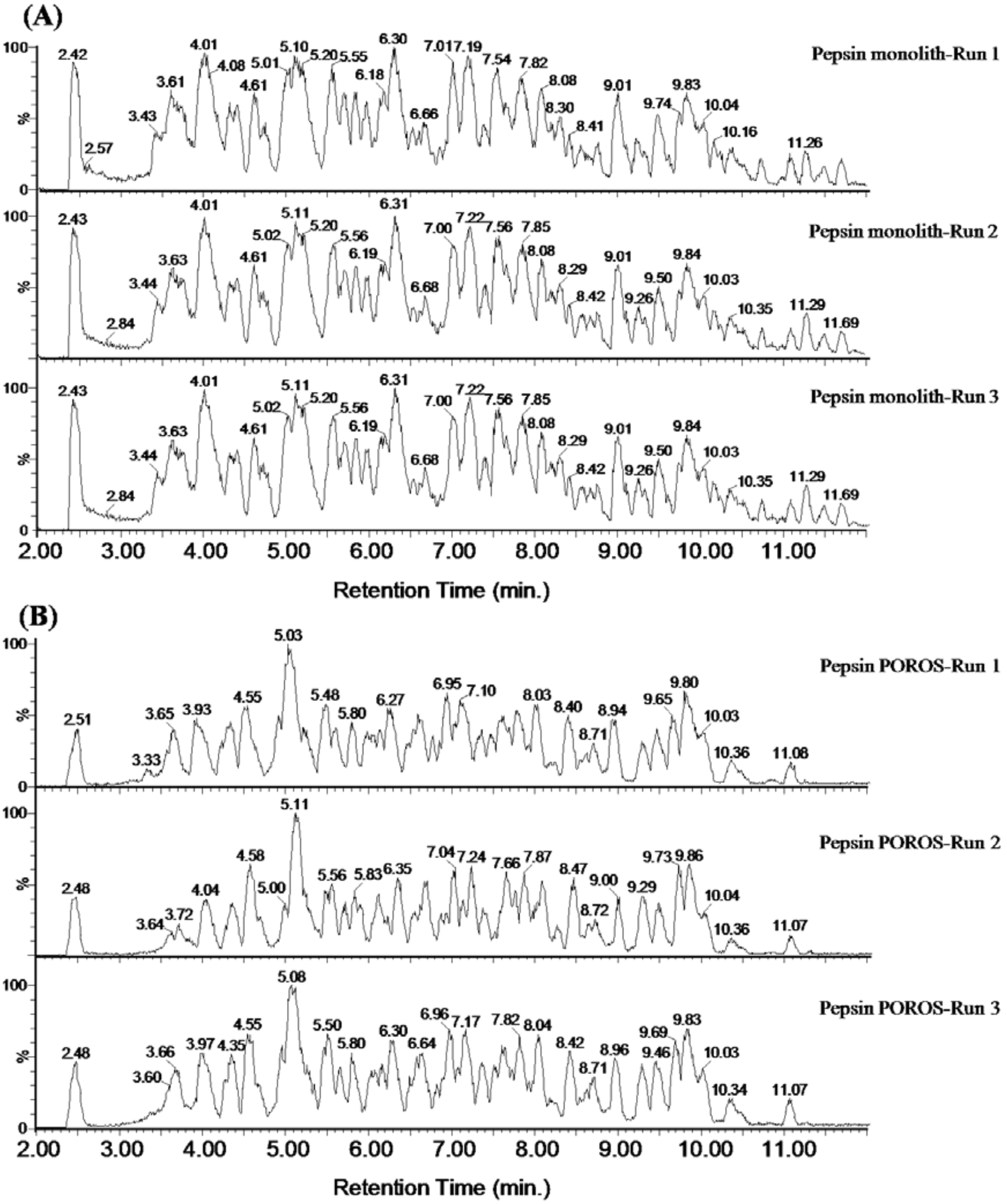

Fig. 3-6 Base peak ion chromatography of IgG and its processed products digested by (A) immobilized pepsin monolith and (B) immobilized pepsin POROS on on-line system of UPLC-ESI-MS/MS in positive ESI mode

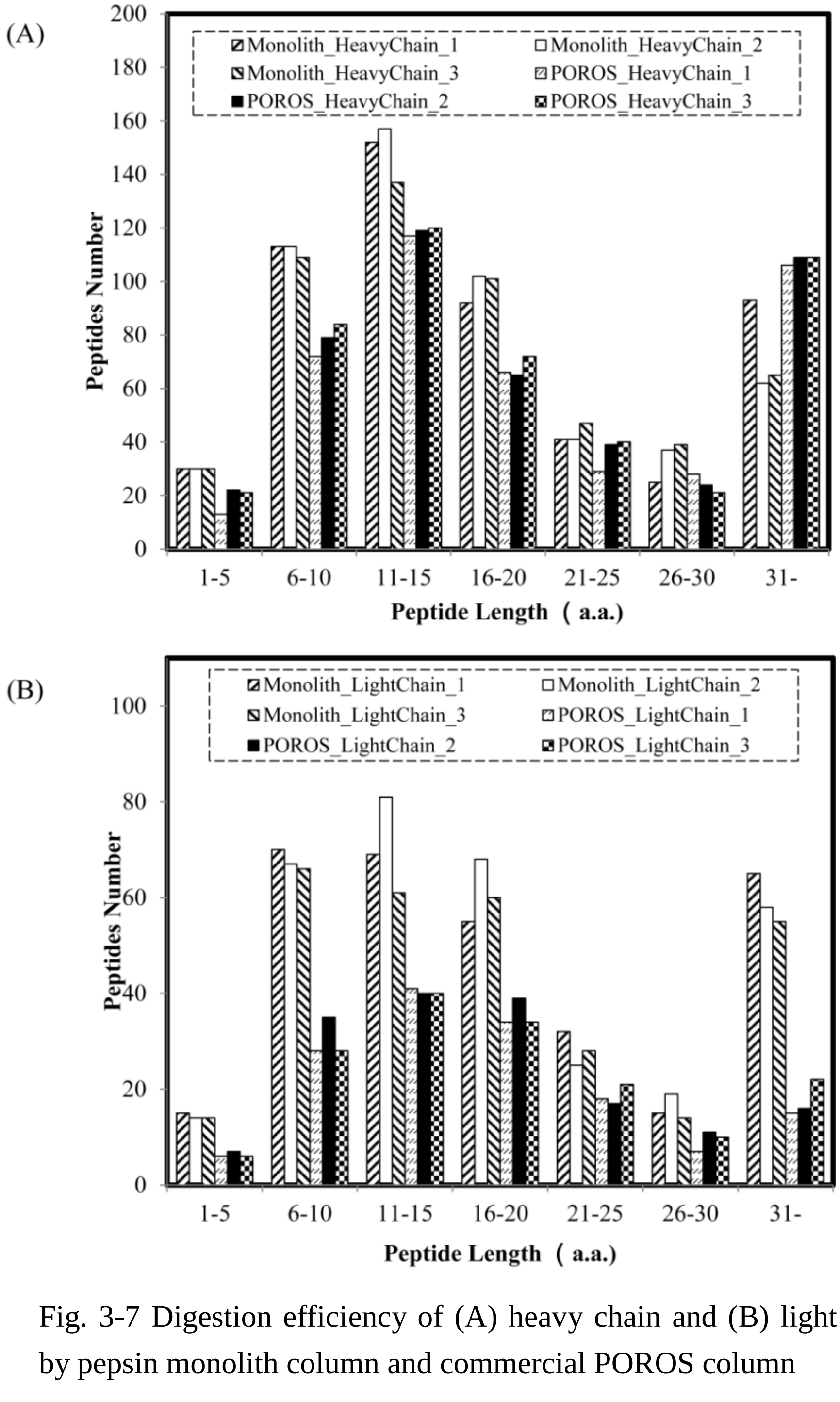

Fig. 3-7 Digestion efficiency of (A) heavy chain and (B) light chain by pepsin monolith column and commercial POROS column

Table 3-2 Efficiency of the pepsin monolith column and the commercial POROS column on IgG digestion

	Peptide coverage (%)		Peptide amount (a.u.)	
	Heavy chain	Light chain	Heavy chain	Light chain
Pepsin monolith-Run 1	99.8	99.5	546	321
Pepsin monolith-Run 2	99.8	99.5	542	332
Pepsin monolith-Run 3	99.8	99.5	528	298
Pepsin POROS-Run 1	99.8	99.5	431	149
Pepsin POROS-Run 2	99.8	99.5	457	165
Pepsin POROS-Run 3	99.8	99.5	467	161

3.4 Conclusion

In conclusion, the PGM monolith with interconnected pores was fabricated by a facile and template-free method, whose pore structure could be readily controlled by preparation conditions, such as cooling temperature and polymer concentration. The epoxy groups on the PGM monolith were modified with aminoacetal followed by acid hydrolysis to obtain the monolith having aldehyde groups. The PGM-CHO monolith was used to immobilize pepsin *via* the reductive amination. The immobilized pepsin showed stability by inhibiting irreversible conformational change of pepsin. The immobilized pepsin was packed into a column and used for UPLC-ESI-MS/MS online protein digestion. The result showed equal to or even better performance than that obtained from the commercial pepsin-immobilized POROS column. It is anticipated that the present efficient sample preparation and the relevant UPLC-ESI-MS/MS online analytical system might provide a promising tool for automated and comprehensive profiling of proteomes and for detailed protein characterization with low cost. Further investigation including the practical application of the present column made of the PGM monolith with immobilized pepsin for online digestion is under way in our laboratory.

References

[1]. Aebersold R and Mann M. *Nature*. 2003;422(6928):198-207.

[2]. Adkins JN, Varnum SM, Auberry KJ, Moore RJ, Angell NH, Smith RD, Springer DL, and Pounds JG. *Molecular & Cellular Proteomics*. 2002;1(12):947-955.

[3]. Lasonder E, Ishihama Y, Andersen JS, Vermunt AM, Pain A, Sauerwein RW, Eling WM, Hall N, Waters AP, and Stunnenberg HG. *Nature*. 2002;419(6906):537-542.

[4]. Florens L, Washburn MP, Raine JD, Anthony RM, Grainger M, Haynes JD, Moch JK, Muster N, Sacci JB, and Tabb DL. *Nature*. 2002;419(6906):520-526.

[5]. Gavin A-C, Bösche M, Krause R, Grandi P, Marzioch M, Bauer A, Schultz J, Rick JM, Michon A-M, and Cruciat C-M. *Nature*. 2002;415(6868):141-147.

[6]. Ho Y, Gruhler A, Heilbut A, Bader GD, Moore L, Adams S-L, Millar A, Taylor P, Bennett K, and Boutilier K. *Nature*. 2002;415(6868):180-183.

[7]. Angel TE, Aryal UK, Hengel SM, Baker ES, Kelly RT, Robinson EW, and Smith RD. *Chemical Society Reviews*. 2012;41(10):3912-3928.

[8]. Marko-Varga G and Fehniger TE. *Journal of Proteome Research*. 2004;3(2):167-178.

[9]. Switzar L, Giera M, and Niessen WM. *Journal of Proteome Research*. 2013;12(3):1067-1077.

[10]. Calligaris D, Villard C, and Lafitte D. *Journal of Proteomics*. 2011;74(7):920-934.

[11]. Chait BT. *Science*. 2006;314:65-66.

[12]. Wu S-L, Hühmer AF, Hao Z, and Karger BL. *Journal of Proteome Research*. 2007;6(11):4230-4244.

[13]. Compton PD, Zamdborg L, Thomas PM, and Kelleher NL. *Analytical Chemistry*. 2011;83(17):6868-6874.

[14]. Zhou H, Ning Z, E. Starr A, Abu-Farha M, and Figeys D. *Analytical Chemistry*. 2011;84(2):720-734.

[15]. Brownridge P and Beynon RJ. *Methods*. 2011;54(4):351-360.

[16]. Lill JR, Ingle ES, Liu PS, Pham V, and Sandoval WN. *Mass Spectrometry Reviews*. 2007;26(5):657-671.

[17]. Sun W, Gao S, Wang L, Chen Y, Wu S, Wang X, Zheng D, and Gao Y. *Molecular & Cellular Proteomics*. 2006;5(4):769-776.

[18]. Peterson DS, Rohr T, Svec F, and Fréchet JM. *Analytical Chemistry*. 2002;74(16):4081-4088.

[19]. Cheng G, Chen P, Wang Z-G, Sui X-j, Zhang J-L, and Ni J-Z. *Analytica Chimica Acta*. 2014.

[20]. Liese A and Hilterhaus L. *Chemical Society Reviews*. 2013;42(15):6236-6249.

[21]. Calleri E, Temporini C, Perani E, De Palma A, Lubda D, Mellerio G, Sala A, Galliano M, Caccialanza G, and Massolini G. *Journal of Proteome Research*. 2005;4(2):481-490.

[22]. Rivera JG and Messersmith PB. *Journal of Separation Science*. 2012;35(12):1514-1520.

[23]. Feng S, Ye M, Jiang X, Jin W, and Zou H. *Journal of Proteome Research*. 2006;5(2):422-428.

[24]. Li Y, Yan B, Deng C, Yu W, Xu X, Yang P, and Zhang X. *Proteomics*. 2007;7(14):2330-2339.

[25]. Li Y, Xu X, Yan B, Deng C, Yu W, Yang P, and Zhang X. *Journal of Proteome Research*. 2007;6(6):2367-2375.

[26]. Kato M, Sakai-Kato K, Jin H, Kubota K, Miyano H, Toyo'oka T, Dulay MT, and Zare RN. *Analytical Chemistry*. 2004;76(7):1896-1902.

[27]. Kim BC, Lopez‐Ferrer D, Lee SM, Ahn HK, Nair S, Kim SH, Kim BS, Petritis K, Camp DG, and Grate JW. *Proteomics*. 2009;9(7):1893-1900.

[28]. Shimazaki Y and Kohno Y. *Analytical Biochemistry*. 2012;422(1):55-57.

[29]. Guiochon G. *Journal of Chromatography A*. 2007;1168(1):101-168.

[30]. Buchmeiser MR. *Polymer*. 2007;48(8):2187-2198.

[31]. Barlow KJ, Hao X, Hughes TC, Hutt OE, Polyzos A, Turner KA, and Moad G. *Polymer Chemistry*. 2014;5(3):722-732.

[32]. Hasegawa G, Kanamori K, Nakanishi K, and Yamago S. *Polymer*. 2011;52(21):4644-4647.

[33]. Walsh Z, Abele S, Lawless B, Heger D, Klán P, Breadmore MC, Paull B, and Macka M. *Chemical Communications*. 2008(48):6504-6506.

[34]. Colard CA, Cave RA, Grossiord N, Covington JA, and Bon SA. *Advanced Materials*. 2009;21(28):2894-2898.

[35]. Zhong H and El Rassi Z. *Journal of Separation Science*. 2009;32(1):10-20.

[36]. Li J, Du Z, Li H, and Zhang C. *Polymer*. 2009;50(6):1526-1532.

[37]. Yao C, Qi L, Jia H, Xin P, Yang G, and Chen Y. *Journal of Materials Chemistry*. 2009;19(6):767-772.

[38]. Kanamori K, Nakanishi K, and Hanada T. *Advanced Materials*. 2006;18(18):2407-2411.

[39]. Bandari R, Knolle W, Prager‐Duschke A, and Buchmeiser MR. *Macromolecular Rapid Communications*. 2007;28(21):2090-2094.

[40]. Ahn J, Cao M-J, Yu YQ, and Engen JR. *Biochimica et Biophysica Acta (BBA)-Proteins and Proteomics*. 2013;1834(6):1222-1229.

[41]. Huhn C, Selman MH, Ruhaak LR, Deelder AM, and Wuhrer M. *Proteomics*. 2009;9(4):882-913.

[42]. Hashem AM. *Bioresource Technology*. 2000;75(3):219-222.

[43]. Wang L, Pan H, and Smith DL. *Molecular & Cellular Proteomics*. 2002;1(2):132-138.

[44]. Mateo C, Fernández-Lorente G, Abian O, Fernández-Lafuente R, and Guisán JM. *Biomacromolecules*. 2000;1(4):739-745.

[45]. Li S, Hu J, and Liu B. *Biosystems*. 2004;77(1):25-32.

[46]. Patel AC, Li S, Yuan J-M, and Wei Y. *Nano Letters*. 2006;6(5):1042-1046.

[47]. Marcsisin SR and Engen JR. *Analytical & Bioanalytical Chemistry*. 2010;397(3):967-972.

Concluding Remarks

This thesis deals with the fabrication of poly(glycidyl methacrylate-co-methyl methacrylate) (PGM) monoliths by thermally induced phase separation(TIPS) method. Through appropriate modification, the PGM monolith can be utilized in various fields. The results obtained through this study are summarized as follows.

In Chapter 1, PGM was synthesized by a conventional radical copolymerization. The unit ratio of MMA and GMA determined by ^{1}H NMR spectroscopy was 89/11. PGM monoliths with three-dimensional continuous interconnected porous structures were successfully fabricated through TIPS method. We found that PGM could be dissolved in the mixture of ethanol and H_2O, both of which are non-solvent of the polymer. This could be explained by the unique cosolvency effect. The morphology of PGM monolith including pore and skeleton sizes was easily tuned by varying the fabrication parameters such as cooling temperature and polymer concentration. The skeleton and pore size increased when the cooling temperature increased and polymer concentration decreased. In addition, the mechanism of the formation of PGM monolith was discussed.

In Chapter 2, I used the epoxide-containing polymethacrylate-based monolith having a well-defined porous structure as a solid support for the immobilization of HRP. The PGM monolith was modified with AADH, EDTAD and NHS to introduce the reactive NHS ester groups, followed by reacting with HRP under mild reaction conditions. The immobilized HRP on the modified PGM monolith showed enhanced thermal stability at 60^{o}C and kept 52% of the original activity after 6 cycles of the reaction. Furthermore, three spacers with different lengths were selected to modified

PGM monolith. Moreover, the spacer structure could reduce the steric interference when HRP was immobilized on modified PGM monolith.

In Chapter 3, the PGM monolith was fabricated *via* the TIPS method described in Chapter 1. The epoxy groups on the PGM monolith were modified with aminoacetal followed by acid hydrolysis to obtain the monolith having aldehyde groups (PGM-CHO). The PGM-CHO monolith was used to immobilize pepsin *via* the reductive amination. The immobilized pepsin showed improved stability by inhibiting irreversible conformational change of pepsin compared with free pepsin. Therefore, the immobilized pepsin was packed into a column and used for UPLC-ESI-MS/MS online protein digestion. The result showed equal to or even better performance than that obtained from the commercial pepsin-immobilized POROS column. It is anticipated that the present efficient sample preparation and the relevant UPLC-ESI-MS/MS online analytical system might provide a promising tool for automated and comprehensive profiling of proteomes and for detailed protein characterization with low cost.

In summary, a polymethacrylate monolith was prepared successfully by using PGM as the precursor *via* TIPS method. The obtained monoliths have unique open-cellular three- dimensional structure and they are applied for enzyme immobilization. PGM monolith has large potential application for biomolecule immobilization.

List of Publications

1. Facile fabrication of poly(methyl methacrylate) monolith *via* thermally induced phase separation by utilizing unique cosolvency

   Shinya Yoneda, Wenjuan Han, Urara Hasegawa, Hiroshi Uyama

   Polymer, 2014, 55, 3212-3216

2. Enzyme immobilization on polymethacrylate-based monolith fabricated *via* thermally induced phase separation

   Wenjuan Han, Yuanrong Xin, Urara Hasegawa, Hiroshi Uyama

   Polymer Degradation and Stability, 2014, 109, 362-366

3. Pepsin immobilization on an aldehyde-modified polymethacrylate monolith and its application for protein analysis

   Wenjuan Han, Mika Yamauchi, Urara Hasegawa, Masanori Noda, Kiichi Fukui, André J van der Vlies, Susumu Uchiyama, Hiroshi Uyama

   Journal of Bioscience and Bioengineering, Accepted

4. Immobilization of horseradish peroxidase on reactive polymethacrylate monolith and its application for phenol removal

   In preparation

Acknowledgments

This study was completed at the Department of Applied Chemistry, Graduate School of Engineering, Osaka University from 2011 to 2014.

First and foremost, I would like to thank my supervisor Professor Hiroshi Uyama, for giving me the opportunity to work on this thesis in this laboratory. I am grateful for his encyclopedic knowledge, constant support and impelling motivation. I benefited from his advice in the course of this research. His positive outlook and faith in my research inspired me and gave me confidence. He is one of the profound influences in my life for my future aspirations.

I would like to thank Professor Tsuyoshi Inoue and Professor Takahiro Kozawa for their tremendous help in revising my thesis.

I wish to express my sincere thanks to Assistant Professor Urara Hasegawa. She provides me a well-rounded knowledge of biology. She always gives me valuable advice whenever I am curious. She is not only a teacher to provide useful academic suggestion, but also a friend to share successful experience, all of which is a significant spiritual support throughout my doctoral research.

I appreciate Dr. André J van der Vlies. He always shares excellent experiment techniques and insightful suggestion without reservation which really helps me a lot. I can not forget the worthy conversation and comment about my research when I needed support.

I am thankful to the support from Professor Kiichi Fukui, Associate Professor Susumu Uchiyama, Dr. Masanori Noda, Ms Mika Yamauchi for their help with the measurement of UPLC-ESI-MS/MS.

I acknowledge Professor Tsuyoshi Inoue, Assistant Professor Eiichi Mizohata for their patient discussion and kindly supply of proteins for my experiment.

I appreciate the support from Professor Susumu Kuwabata, Assistant Professor Taro Uematsu for their kindly helps with the ICP-AES measurements.

I thank Dr. Junji Sakamoto for the valuable discussion and advice on my experiment.

I am grateful to my senior, Dr. Yuanrong Xin, who gives me support both in academic and in life. Her wisdom and humor add more joy into my tough life as a doctor.

I am much obliged to Ms. Xiaoxia Sun, Ms. Sung-Bin Park, Mr. Masaki Moriyama, Mr. Guowei Wang, Mr. Boxing Zhang, Mr. Tengjiao Wang, Ms. Hyunhee Shim, Mr. Qinghui Zhang, Mr. Haotian Wang and all the members in Uyama laboratory. Because of their support, help and friendship, I could not imagine the hard life during the three years.

I wish to express the gratitude the help from Ms. Tomoko Shimizu and Ms. Yoko Uenishi for their warmly help to overcome my various difficulties.

I am indebted to Professor Changyu Shen, Professor Chuntai Liu and Associate Professor Guoqiang Zheng in Zhengzhou University for their encouragement and support to pursue my doctoral degree overseas.

Thanks to the China Scholarship Council (CSC) for providing finical support on my academic study and stay in Japan.

I would like to express particular appreciation to my family. My father, Shouli Han and my mother, Cuihua Guo, gave me birth and rised me with such unconditional love and support in all of my life’s endeavors. They are always there for me no matter

what. I also thank my fiancé, Dr. Xiaofeng Wang for his support, love and friendship which make everything worthwhile. I additionally thank my wonderful brother, Wenfu Han and all the rest of my extended family for their love and friendship.

To anyone else who has known me and helped over the years, thank you. I am very blessed.

October 2014

Wenjuan Han